The Permian Cornubian Granite Batholith, SW England; Part 2: Gravity anomalies, structure, and state of isostasy

A. B. Watts[1], C. Xu[1,2], M. P. Searle[1], C. Jurkowski[1], R. K. Shail[3]

[1]Department of Earth Sciences, University of Oxford, South Parks Road, Oxford, OX1 3AN

[2]Key Lab of Submarine Geosciences and Prospecting Techniques, Ministry of Education, and College of Marine Geosciences, Ocean University of China, Qingdao, China, 266100

[3] Camborne School of Mines, Department of Earth and Environmental Science, University of Exeter (Penryn campus), Penryn, Cornwall, TR10 9FE

Abstract

A new compilation of Bouguer gravity anomaly data has been used, together with forward and inverse modelling, to reappraise the structure, volume, and state of isostasy of the Cornubian batholith of SW England. We show the upper 2-3 km of the plutons that comprise the batholith slope outwards, are on average ~10-11 km thick, connected at depth, and appear to be underlain by roots which protrude into the middle crust. We estimate the batholith volume as within the range 76,367 ± 17,286 km^3, significantly larger than previous estimates. Granite outcrops correlate with elevated topography and mass balance calculations show that the mass deficiency of the granites relative to their host metasedimentary rocks is approximately equal to the mass excess of the topography relative to air. The existence of roots beneath individual plutons are in general agreement with predictions of an Airy model of isostasy and a depth of compensation that is within the crust rather than at the Moho. In addition, a middle crust compensation depth is compatible with the origin of the granites by heating and melting of pre-existing metasedimentary rocks and with data from experimental rock mechanics which suggest that at the melting temperature and pressure of granites, deformation is plastic and is controlled by glide of dislocations. During pluton emplacement the middle crust would therefore have acted as a mechanically weak layer, effectively decoupling the topography from any support it might otherwise have received from the lower crust and/or upper mantle.

INTRODUCTION

It has been more than 50 years since the classic studies of M. H. P. Bott and colleagues (Bott et al., 1958; Bott and Scott, 1964; Holder and Bott, 1971) on gravity anomalies and the structure and mechanisms of emplacement of the Cornubian granites of SW England. These studies showed that the Permian granite outcrops of Cornwall and south Devon are associated with a +250-km-long, 20-40-km wide belt of Bouguer gravity anomaly 'lows' of -40 to -60 mGal and that the anomalies were caused by the relatively low density of the granites compared to that of their metasedimentary host rocks. Using limiting depth methods and the gravity effect of simple two-dimensional shapes (e.g., rectangular block, vertical cylinder). Bott et al., (1958) and Bott and Scott (1964) argued that individual plutons and stocks formed part of the roof zone of an outward sloping batholith which had a density contrast with its host metasedimentary rocks of about -140 kg m^{-3} and extended to depths of at least 8 km and, possibly, to 20 km below present-day sea-level. The minima of the 'lows' correlate with granite outcrops which, in turn, are associated with the most elevated topography. Bott et al., (1958) and Bott and Scott (1964) speculated that the thickness of granite and the height of topography were linked, and that some form of isostatic balance existed between the upward acting forces associated with the emplacement of the low-density granite and the downward acting forces associated with the topography. The depth of compensation they inferred was probably within the crust at a depth 10-15 km which Bott et al., (1958) noted was unusually shallow.

Since these pioneering studies, the increase in availability of onshore and offshore gravity data, together with the development of more sophisticated forward and inverse modelling techniques, have resulted in a better understanding of the sub-surface structure of the Cornubian granites. Tombs (1977), for example, used the three-dimensional polygon methods of Talwani and Ewing (1960) and Cordell and Henderson (1968) to calculate the gravity effect of the granites and compare them to the observed gravity anomaly. By manually adjusting the polygons they found the best fit between calculated and observed Bouguer gravity anomalies was for depths to the deepest base polygon of 20, 15 and 10 km for the Dartmoor, Land's End and the Scilly Isles granites respectively assuming a regional background gravity field (i.e., that part of the field not caused by the granites) of +30 mGal (1 mGal = 10^{-5} m s^{-2}) and a density contrast between the granites and host rocks of -100 kg m^{-3}. Each causative body sloped outwards to a depth of at least 2 km. Tombs (1977) argued that the apparent thinning of the granite batholith from Dartmoor westward to Land's End was not caused either by lateral density changes of the granite, as a local isostatic model would predict, due to the uniformity in composition of the granites, or by lateral density changes of the metasedimentary rocks that host them, due to it changing the regional background field. Al-Rawi (1980) used two-dimensional methods and a range of density contrasts from -100 to -150 kg m^{-3} to estimate the depth to the base of the granites as in the range 9-16 and 12-22 km for Land's End and Dartmoor respectively. Willis-Richards and Jackson (1989) used a similar approach as Tombs (1977) to construct a model for the granites between Land's End and Dartmoor assuming a range of density contrasts from -110 to -130 kg m^{-3} and a regional background of +25 to +35 mGal, confirming that the granites were connected at depth with 'saddles' of sub-surface granites separating the main plutons. Willis-Richards and Jackson (1989) showed that Sn-Cu-Pb-Zn mineralization was generally coincident with the axis of the modelled batholith, estimating its volume as 68,000 km^3. Finally, Al-Rawi (1980) used gravity anomaly data to suggest the base of the Land's End granite was at a depth of ~8 km assuming a density contrast of -200 kg m^{-3}. They used regional gravity and magnetic anomaly data to suggest the granite was underlain by a 6 km thick lower crustal body with a density contrast with its surroundings of +200 kg m^{-3} and a remanent magnetization contrast of 1.7 × 10^5 A m^{-1}. They argued that the combined gravity effect of the Land's End granite and the lower crustal body could explain both the -20 mGal Bouguer anomaly 'low' over the granite and the +30 mGal anomaly regional background field in flanking regions.

Edwards (1984), among the first to consider the gravity field offshore Cornwall, used a two-dimensional method, a density contrast of -130 kg m^{-3} and a regional field of +40 to +45 mGal to show that the NE-SW trending Haig Fras ridge and the seafloor south-west of the Scilly Isles were underlain by a granite batholith up to 7-12 km thick which in both cases had intruded into host metasediments. He found that Haig Fras was not, however, connected to the Cornubian batholith but was separated from it by a sedimentary basin (the Haig Fras sub-basin) which is infilled by Permo-Triassic and younger sediments.

Seismic refraction and wide-angle reflection data are generally supportive of the results from gravity modelling that the granite outcrops represent a batholith. Holder and Bott (1971) acquired an 'along axis profile' of the batholith by shooting at sea along a line south-west of the Scilly Isles and between the Scilly Isles and Land's End into seismic recording stations located on the Scilly Isles, Land's End, Carnmenellis, Bodmin and Dartmoor granites. They identified a *Pg* arrival at all stations except Dartmoor which they interpreted in terms of a 10-12 km thick granitic upper crust with a *P*-wave velocity of 5.85±0.05 km s^{-1} implying, according to the *P*-wave velocity and density empirical relationship of Christensen and Mooney (1995), a density of 2648±18 kg m^{-3}. *PmP* arrivals at all stations and *Pn* arrivals at all stations except Carnmenellis indicate Moho at a depth of ~27 km. Brooks et al. (1984) subsequently used shots at sea into seismic recording stations spaced 2-3 km apart along 6 ‘dip profiles’ (i.e., profiles that are of high angle to the batholith axis) of the main granites, except Land’s End and St. Austell. They identified arrivals from 3 wide-angle reflectors on their Lines 4, 5 and 6 which crossed the Carnmenellis, Bodmin and the western edge of Dartmoor granites: R1 gave a depth at 8 km depth and a *P*-wave velocity down to an assumed horizontal reflector of 5.90 km s^{-1} which they interpreted as originating from the interior of the granite, R2 at a depth of 10-15 km and a velocity down to an assumed horizontal reflector of 5.75 km s^{-1} which they interpreted as from the base of granite and, R3 at a depth of 27-30 km and a velocity down to the assumed horizontal reflector of 6.20-6.35 km s^{-1} which they interpreted as Moho.

During 1981-1985 the British Institutions Reflection Syndicate (BIRPS) used a towed airgun array source and a 3-km-long multichannel hydrophone ‘streamer’ to acquire a number of seismic reflection profiles offshore Cornwall and south Devon as part of its South-West Approaches Traverse (SWAT) and Western Approaches Margin (WAM) projects (Alexander et al., 2019; ECORS, 1986; Klemperer and Hobbs, 1991; Prive, 1986). SWAT 6 crossed the southwest extension of the Scilly Isles pluton and SWAT 5 crossed the Haig Fras plutons. No reflections were observed from within the regions of granite. However, the reflective lower crust, which is characteristic of the Variscan crust of northwest Europe (e.g., Meissner, 1986), and may represent sharp lithological boundaries (Warner et al., 1994) was observed to thin beneath the plutons on both traverses. Gravity and seismic modelling (Prive, 1986) suggest the Haig Fras granite on SWAT 5 was more a vertical intrusion, in contrast to the Scilly Isles granite on SWAT 6 which was more an outward sloping pluton. Both modelled bodies had a base which extended to depths of ~10 km.

More recently, Taylor (2007) used gravity anomaly data to question a plutonic origin for the Cornubian granites. He proposed instead a model of multiple sill emplacement, predicting an average granite thickness of 3.5-3.7 km for Carnmenellis, St. Austell and Bodmin and 9 km for Dartmoor, assuming a density contrast of -130 kg m^{-3}. These thicknesses are significantly less than those deduced by Tombs (1977), Al-Rawi (1980) and Willis-Richards and Jackson (1989) using similar density contrasts. However, the study of Taylor (2007) assumed a regional background field of ~+10 mGal for Carnmenellis, St. Austell and Bodmin, significantly lower than that assumed in previous studies (+25 to +45 mGal). By lowering the regional background field Taylor (2007) had, in effect, only modelled the shortest wavelengths of the Bouguer gravity anomaly 'low' where it coincides with the granite outcrop. As a result, the modelled bodies of Taylor (2007) mostly dip inwards rather than outwards and are low in volume (~40,000 km^3 according to Williamson et al. 2010) compared to previous estimates. Another difficulty, recognised by Taylor (2007), is that it leaves unexplained the remaining longer wavelengths of the 'low' since a low regional background field implies a mass excess that flanks the mass deficiency of the granites which was not accounted for in the Taylor (2007) models.

The Cornubian granites have long been of interest for their association with mineral resources such as tin, tungsten, copper, lead and zinc and, most recently, lithium and for the role they might have played in the Variscan orogeny of northwest Europe. The aim of this paper is to reappraise the gravity field of the SW England region and its interpretation in terms of the sub-surface structure of the granites. We show, using a new compilation of onshore and offshore gravity anomaly data and a range of modelling approaches, including two-dimensional and three-dimensional and forward and inverse techniques, that gravity data are consistent with a 'hybrid' model which has elements of both a pluton and sill model for the origin of the granites. The evidence suggests that the upper 2-3 km of each pluton that comprise the batholith has outward slopes, the steepest of which are aligned along Variscan trends. Moreover, the batholith has an average thickness of 10-11 km and appears to be underlain by roots which protrude downwards into the middle crust. The total volume of the modelled batholith is larger than previous estimates and our most likely interpretation is that the granites were emplaced individually as plutons in the upper crust either by sill emplacement, dyking or some combination of these processes due to some form of heating and melting of amphibolite facies rocks in the middle crust.

GEOLOGICAL SETTING

At least two parallel granitic batholiths are present in southwest England, the first the Cornubian batholith is of Permian age, and extends along the mainland of Cornwall and south Devon, and the second extends along the Haig Fras ridge off the north coast of Cornwall. The Cornubian batholith extends from west of the Scilly Isles in the southwest to Dartmoor in the northeast confiming the hypothesis originally advanced by De La Beche (1839) of a single continuous batholith with numerous smaller stocks. Six major granite bodies are exposed in Cornwall and south Devon including the Scilly Isles, Land’s End, St. Austell, Carnmenellis, Bodmin and Dartmoor granites, as well as several smaller stocks such as St. Michael’s Mount (Penzance), Tregonning-Godolphin, Cligga Head, Kit Hill, Hemerdon and Castle an Dinas. U-Pb zircon and monazite dating shows that the Cornubian granites are Early-Middle Permian ranging between ~295-275 Ma (Chen et al., 1993; Chesley et al., 1993; (Smith et al., 2019). The submarine Haig Fras granites have been sampled and dredged (Exley, 1966; Edwards, 1984), dated as ~277 ± 10 Ma (Smith et al., 1965), and surveyed using a towed gamma-ray spectrometer (Jones et al., 1988).

The Cornubian granites are heterogeneous and display significant mineralogical, textural, and chemical variations within a single pluton. They are generally classified as crustal melt S-type granites with two-mica and biotite- tourmaline- K-feldspar granites dominating (Exley and Stone, 1982; Stone and Exley, 1985; Willis-Richards and Jackson, 1989; Floyd et al., 1993; Chappell and Hine, 2006; Simons et al., 2016; Simons et al., 2017; Smith et al., 2019; Searle et al., Part 1). The granites are believed to have derived from previously enriched continental crust, with a complete spectrum of processes from magmatic to hydrothermal and truncate regional folds, faults and cleavage, formed as a result of Late Devonian and Carboniferous Variscan deformation (Shail et al., 2003; Hughes et al., 2009).

The granites are peraluminous and were most likely derived by partial melting of a feldspathic pelite-psammite sedimentary source (Chappell and Hine, 2006; Müller et al., 2006; Simons et al., 2016; Simons et al., 2017). The oldest granites (300-288 Ma) are the two-mica granites (e.g., Scilly Isles, Bodmin and Carnmenellis) and muscovite granites (Hemerdon), and the younger granites (284-274 Ma) are the composite biotite and tourmaline granites of Dartmoor, St. Austell, and Land's End (Smith et al., 2019). Simons et al. (2016) proposed a two-stage model where the older granites formed by muscovite-dominated dehydration melting at Pressure-Temperature (P-T) conditions of 800-730ºC and >500 MPa or a depth of ~20 km. Later melting with increasing temperature and lowering pressure resulted in biotite-dominated melting and generation of the biotite granites which fractionated to form the tourmaline granites. U-Pb zircon and monazite geochronology indicate ages from zircon cores are 288.9 ± 5 Ma and 286.4 ± 5 Ma (Smith et al., 2019), corresponding to ages of two-mica and muscovite granites (e.g., Carnmenellis, Bodmin, Hemerdon). Zircon rim ages (277.74 ± 0.33 Ma and 278.35 ± 0.35 Ma (Smith et al., 2019) correspond to the later biotite and tourmaline granites (e.g., Dartmoor, St. Austell and Land's End granites).

The granite batholiths of Cornwall and south Devon intrude mainly Devonian and Lower Carboniferous metasedimentary and metavolcanic rocks (Exley and Stone, 1982). The sedimentary and associated volcanic rocks probably formed in a volcanic (extensional) rifted margin setting at the northern edge of the Rheic Ocean (Alexander et al., 2019) in the southern hemisphere. Obduction of the Lizard ophiolite oceanic crust and upper mantle onto the continental margin of Avalonia marked the beginning of the closure of the Rheic Ocean and the onset of the Variscan orogeny. Compressional deformation of the rifted margin sedimentary and volcanic rocks involving thrusting and folding (e.g., Williams and Chapman, 1986; Shail and Leveridge, 2009) continued through the Devonian and Carboniferous. According to Shail et al. (2003) the granites of SW England were emplaced in the early Permian during a ~30 Myr-long extensional phase that followed culmination of the Variscan orogeny in the Late Carboniferous.

GRAVITY, BATHYMETRY AND TOPOGRAPHY DATA

The gravity, bathymetry and topography data used in this study have been compiled from several sources (Figure 1). They include a British Geological Survey (BGS) Land Gravity 'point' data set, an EMODnet bathymetry and OpenStreetMap topography grid, and a satellite-derived V28.1 free-air gravity anomaly grid. The BGS data is based on 4756 gravity measurements in Cornwall and south Devon and has been referenced using the Geodetic Reference System 1967, the International Gravity Standardisation Net 1971 and the National Gravity Reference Net 1973. The EMODnet grid is a 0.0625 × 0.0625-minute bathymetry and topography grid (~ 115 × 115 metre) based on single beam and multibeam (swath) sonar surveys, Hydrographic Office lead-line surveys, and satellite-derived data offshore and terrestrial OpenStreetMap data onshore. The satellite-derived V28.1 gravity grid is a 1 × 1 min grid (~1.85 × 1.85 km) based on ERS-1 and GEOSAT and, since 2010, data derived from the CryoSat-2, Jason-1, Jason-2, and SARAL/AltiKa satellite altimeter missions. The satellite-derived gravity data is estimated to be accurate to ~1–2 mGal (Sandwell et al., 2019).

The 'point' and gridded data sets are of variable spacing, but for interpretation we require a single grid for the gravity and bathymetry and topography data. After several tests, we selected a grid interval of ~250 m for the gravity data set and ~115 m for the bathymetry and topography data sets. These grid intervals were wide enough to avoid aliasing and narrow enough to resolve quite small features in both the gravity anomaly and bathymetry and topography data (Figure 1). The reduction of the offshore free-air gravity anomaly data set to Bouguer gravity anomalies assumed that rock of density 2700 kg m^{-3} displaced sea water of density 1030 kg m^{-3}. The same rock density was assumed by the BGS in their reduction of the onshore data.

Figure 1a shows a Bouguer gravity anomaly map of the south-west England region. The map is dominated by several intense 'lows' which are flanked by a broad region of 'highs'. The 'lows', which reach amplitudes of up -40 to -60 mGal, form a linear belt of negative anomalies that extend from the Scilly Isles in the southwest to Dartmoor in the northeast. The 'highs', which reach amplitudes of 30 to 45 mGal form part of a long wavelength free-air gravity anomaly 'high' associated with much of western Britain (Al-Kindi et al., 2002). The topography map (Figure 1b) shows localized highs of up to > 300 m above sea-level which correlate closely with the Bouguer gravity anomaly ‘lows’. Offshore north Cornwall, there is a region of relatively shallow seafloor bounded by ‘cliffs’ (Evans, 1990, figure 10), the Cornubian platform, which is widest west of the Cligga Head granite (Figure 1a) where it correlates with an offshore extension of the Bouguer gravity anomaly ‘lows’.

GRAVITY MODELLING

Two-Dimensional Models

The first step in gravity interpretation is to separate the anomalies associated with the granites from the regional background field. To carry this out we sought a regional that could be easily reproduced by filtering the observed Bouguer gravity anomaly. Various filters were tested, and it was found that a median filter (width = 300 km) (Figure 2a) most satisfactorily removed the gravity anomaly ‘lows’ while at the same time preserved the flanking gravity anomaly ‘highs’. The filtered gravity anomaly increases gently from +27.5 mGal in the northeast to +37.5 mGal in the southwest and, significantly, individual contours show no relationship with the general northeast-southwest trend of the main granite outcrops (Figure 2b). The increase is long wavelength, and we speculate that it may be related, at least in part, to a thinning of the continental crust. Figure 2c shows the residual Bouguer gravity anomaly obtained by subtracting the filtered anomaly from the observed Bouguer gravity anomaly. This anomaly, which reveals gravity ‘lows’ of up to -40 to -60 mGal, is clearly directly related to the granite outcrops and was therefore selected as a basis to interpret their detailed sub-surface structure.

We first sampled the Bouguer gravity anomaly grid along a set of 8 profiles orthogonal to the central part of the linear belt of negative anomalies (Figure 2a,c). The profiles, which intersect the outcrops of the Tregonning-Godolphin, Carnmenellis, St. Austell and Bodmin granites, were then ensemble averaged. This is a spectral technique (e.g., Bassett and Watts, 2015) that obtains the most 'typical' profile by suppressing features not common in a set of profiles and enhancing the features that are. The results of ensemble averaging the 8 Bouguer gravity anomaly profiles, together with the profiles used, are shown in Figure 3.

We used a matrix inversion technique (Tanner, 1967) to interpret the ensemble averaged profile in Figure 3. This technique, which determines the geometry of a causative body directly from an observed gravity anomaly, is based on Green's equivalent layer theorem which states that any gravity anomaly can be represented by an equivalent surface mass distribution. By assuming a uniform density contrast with its surroundings, a surface mass can then be represented by a simple shape such as a rectangular block. The base of the block is then iteratively adjusted until a satisfactory fit is achieved between observed and calculated gravity anomaly. The technique, which was modified by Laving (1971) to produce smooth body outlines, assumes that in the case of an outward sloping body that the depth to one point on the upper surface of the body is known and that the lower surface is flat.

Figure 4 shows the application of the matrix inversion technique to the ensemble profile in Figure 3 after removal of the regional background field. To avoid 'trailing errors' an additional regional that increased by 3 mGal along the profile was applied, as illustrated by the thin dash line in Figure 4. The figure shows the ensemble profile can be explained well by an outward sloping granite body with a density contrast of -150 kg m^{-3} with its surroundings and a flat base at a depth of ~10 km. This depth is in excellent agreement with the thickness of the granitic upper crust estimated by Holder and Bott (1971) based on *Pg* arrivals at seismic recording stations at Carnmenellis and Bodmin.

The Root Mean Square (RMS) difference between the observed residual and calculated Bouguer gravity anomalies is 0.5 mGal which is small compared to the amplitude of the observed residual gravity anomaly of ~-50 mGal (i.e., ~0.1%). Within the region of granite outcrop the granite depth is < ~2 km so the granite body clearly extends well beyond the granite outcrop.

The models of Taylor (2007) for the Dartmoor, Bodmin and Carnmenellis granites are characterised by inward sloping sill-like bodies with roots that protrude downwards. Such a root may represent frozen granite melt zone and/or some form of isostatic compensation for the topography created by rising granite magma. It is instructive therefore to consider the gravity effect of such a root. Figure 5 shows a simple model of a root that underlies the main granite batholith modelled in Figure 4 and protrudes downward into the middle crust. The gravity effect of the root, assuming a density contrast of -150 kg m^{-3} with the surroundings, is about 1/5 of the amplitude of the observed and calculated residual Bouguer gravity anomaly but is long in wavelength. There might be some 'trade-off' therefore between the gravity effect of the batholith and its root: a deeper root could lead to thinner batholith while a shallower root could lead to a thicker batholith.

We assumed in the modelling thus far that the granite batholith is outward rather than inward sloping. As shown by Bott (1962), it is possible to distinguish between these slopes by consideration of the second horizontal derivative of the gravity anomaly. Figure 6 shows, for example, that an outward sloping mass deficiency (i.e., a body of negative density contrast with its surroundings) is associated with a positive second horizontal derivative over its upper surface and a negative second horizontal derivative over its flank. The intensity of the positive derivative varies with the outward slope: the more positive the derivative the steeper the slope. A vertical sided body has a positive derivative that is the same amplitude as the negative derivative while for bodies with outward slopes the positive derivative is generally larger in amplitude than the negative derivative.

The model in Figure 6 is an idealized one so it may be difficult to apply Bott's criterion to actual gridded gravity anomaly data sets because of geological complexity due to lithological variations and because of artifacts that arise, for example, from combining onshore and offshore data sets. Nevertheless, Figure 7 shows intense positive second horizontal derivatives (dashed black lines, Figure 7) dominate the edges of the granite outcrops at Dartmoor, Bodmin, St. Austell, Carnmenellis and Land's End. The positive derivatives are flanked, in many cases, by negative derivatives (dashed white lines, Figure 7). Interestingly, the intense positive and negative derivatives, and hence the steepest slopes of the outward sloping granite bodies, have a generally west-east trend, similar to that of the Devonian and Carboniferous sedimentary basins forming the volcanic rifted margin of the Rheic Ocean (Shail and Leveridge, 2009). The east-west trend apparently influenced orientation of ophiolite obduction in the Middle Devonian and thrusting and folding of the rifted margin sediments through to the Late Carboniferous and subsequent extensional reactivation during the Early Permian (Shail and Leveridge, 2009). The trends of the second horizontal derivatives therefore suggest that granite emplacement in the Early Permian may have been controlled in some way by these pre-existing Variscan structures

We also assumed in modelling that the density contrast between the granites and surrounding metasediments is uniform and -150 kg m^{-3}. Such a contrast is consistent with the >400 density measurements of Bott et al. (1958) who showed that the average density of the granites and the host metasedimentary rocks are 2609 and 2750 kg m^{-3} respectively. However, density variations due to mineralogical, chemical and lithological changes can be expected in both the granites and surrounding metasedimentary rocks. Taking such variations into account, Bott et al., (1958) estimated that the average densities for the granite and metasedimentary rocks might be subject to errors of up to ±30 kg m^{-3}. The error suggest density contrasts that could range from approximately -180 to -120 kg m^{-3}.

The effect of variations in density contrast on the geometry of a granite batholith is illustrated in Figure 8 for the Carnmenellis granite. The figure shows the depth to the base of the granite changes significantly with different density contrasts: depth decreases with increase in density contrast. We found that for density contrasts less than -140 kg m^{-3} the matrix inversion method is unstable and could not find an outward sloping body with a flat base that fit the observed Bouguer gravity anomaly.

One way to constrain the density contrast is to compare the calculated depth to the upper surface of a model to the observed depth in a mine. At South Crofty mine, for example, the contact between the host metasediments and the granite has been reported to be at variable depths of ~0.15 km below sea-level where the apparent dip is to the northwest (Shail pers. Comm.). This is in close agreement with the model prediction based on a density contrast of -200 kg m^{-3} (Figure 9). Unfortunately, we were not able to distinguish, in this case, between different density contrasts. Smaller density contrasts (e.g., > -140 kg m^{-3}) were unstable and larger contrasts (e.g., < -200 kg m^{-3}) required a similar depth to the top of the granite as did the -200 kg m^{-3} case.

Finally, we assumed in the modelling two- rather than three-dimensions. The two-dimensional assumption has been used in previous studies and should be appropriate for a causative body significantly longer (i.e., ~4 times) than its width. While the Cornubian granites appear to be connected at depth, their shallow structure varies and there are depressions or 'saddles' in the upper surface of the granites between the main plutons. A two-dimensional assumption does not consider such saddles and will tend therefore to overestimate the mass of a body and cause the depth of the granite to be underestimated. Figure 9, which compares the structure of the granite based on a two-dimensional assumption to the case of a three-dimensional structure approximated by end-effect corrections (e.g., Bott, 1960), shows this to be the case for the South Crofty mine profile. A three-dimensional structure assuming the granite has a circular structure with a radius of ~22 km predicts a depth to the base of the granite of 11.1 km, which is 2.3 km deeper than is predicted for the two-dimensional case.

Three-Dimensional Model

There are indications that even though the batholiths are connected at depth and align along a generally linear northeast-southwest trend the best modelling approach would be a three-dimensional rather than a two-dimensional one with or without end-effect corrections. The evidence is the roughly circular outcrop and cupola origin of at least some of the granites (e.g., Carnmenellis, Bodmin) and the fact that the steepest slopes of the causative granite bodies inferred from the derivative map have a Variscan trend (e.g., Figure 7) which are highly oblique to the linear trend.

To address three-dimensionality we used the iterative method of Götze and Lahmeyer, (1988) and Schmidt et al. (2010) referred to as IGMAS+**.** This method rapidly calculates the three-dimensional gravity effect of a causative body by constructing a series of triangular polygonal interfaces from vertical sections and by replacing the volume integral in the formula for the gravity effect of a single interface by the sum of one or more-line integrals. The structure along an individual vertical section is adjusted until a satisfactory fit is obtained between the calculated and observed Bouguer gravity anomaly.

We inputted the residual Bouguer gravity anomaly grid of Figure 2c into IGMAS+, enlarging it somewhat southwest of the Scilly Isles to include the offshore Haig Fras granite. The enlarged area is shown in Figure 10 together with the Bouguer gravity anomaly, regional background field and the residual Bouguer gravity anomaly. Thin black lines in Figure 10a show the 79 vertical sections (spaced ~4.4 km apart) used in the modelling. Thick white lines locate the 8 vertical sections selected in Figure 11a,b for the comparison of the observed and the 'best fit' calculated Bouguer gravity anomalies. In each section, two uniform density layers are adjusted: an upper layer comprising the mainly outward sloping part of the batholith and a lower layer comprising a root that protrudes into the middle crust. Both layers were assumed to be of a uniform density contrast of -150 kg m^{-3} with their surroundings. As Figure 8 shows for the two-dimensional case, increasing the contrast will reduce the thickness of the granite body while decreasing it increases the thickness.

The existence of a root beneath the batholiths is in interesting consequence of modelling. We found a root to be necessary in most, but not all sections. The gravity effect of the root is relatively long in wavelength (e.g., Figure 5) and ensures that the uppermost part of the granite is confined to the region of outcrop while at the same time maintaining the depth of the main batholith at the seismically constrained depth of ~10 km and helping to produce a close fit in flanking regions.

Figures 11a,b show that an excellent fit is achieved using the three-dimensional IGMAS+ iterative method between the residual Bouguer gravity anomaly and the calculated anomaly in the region of the granite bodies in both onshore and offshore regions. The RMS difference of the overall comparison is better than 1.5 mGal which is comparable to that achieved using the two-dimensional matrix inversion method (e.g., Figures 8 and 9).

The final step in the modelling was to use the vertical sections to construct a grid of the depth to the top and bottom surfaces of the granites. We assumed a grid interval of 500 × 500 m which is twice the grid interval of the input residual Bouguer gravity anomaly. Depths between vertical sections were interpolated using a "voxelization" gridding technique (Götze and Lahmeyer, 1988; Schmidt et al., 2010) and the grid masked to isolate the granite bodies from the Permo-Triassic sediments of the flanking Haig Fras sub-basin as well as the sediments of the South-western Approaches and Celtic Sea basins.

A perspective plot of the masked grid of the top and bottom of the granite bodies is shown in Figure 12. The figure demonstrates the remarkable continuity of both the Cornubian and Haig Fras granite bodies at depth. The two bodies are not, however, connected. Also shown are the roots that protrude into the middle crust which are best developed beneath Dartmoor where, interestingly, the topography is highest. More modest roots exist beneath the Bodmin, Carnmenellis and Land's End granites which are of lower topography than Dartmoor.

The spatial extent of the granite bodies and their relationship to the coastline, granite outcrops and topography and bathymetry is shown in planform in Figure 13. The figure reveals a close correlation between the thickest granite and the outcrop of the main plutons. The main exception is Carnmenellis, where the maximum thickness appears to be to the north of the outcrop. The figure also shows the relationship between the outer limit of the granite and the coastline and the bathymetry and topography. The southern outer limit of the Cornubian batholith, for example, closely follows the coast of Cornwall while the northern outer limit crosses south Devon and then continues offshore where it follows the outer cliff (Evans, 1990) edge of the shallow insular shelf of the Cornubian platform. The region between the southern and northern outer limits therefore encompasses the topographic highs associated with the plutons, the widest part of the shallow insular shelf offshore the north coast of Cornwall and the shallows that flank the Scilly Islands and Seven Stones reef.

DISCUSSION

Volume And Mass Estimates

The three-dimensional grid used to construct Figure 12 can be used to compute both the volume and mass (mass is the product of volume and density) of the two main granite bodies. The volume and mass of the Cornubian batholith, for example, is 85,730 km^3 and

2.270×10^{17} kg (2.270×10^{14} metric tons) respectively. These estimates include the roots that protrude into the middle crust.

As discussed in Searle et al. Part 1, the roots probably comprise a frozen melt/mush zone made up of granite and migmatite. In this case, then there will be less granite in the root which will reduce its volume and mass. For example, a 50% granite 50% migmatite mix reduces the volume and mass to 76,367 km^3 and 2.022 $\times10^{17}$ kg (2.022×10^{14} metric tons) respectively. The volume and mass of the offshore Haig Fras granite are significantly smaller than the Cornubian batholith. The volume and mass of the former batholith are 14,414 km^3 and 3.817×10^{16} kg (3.602×10^{13} metric tons) respectively and the reduced volume and mass after correcting for root composition in this case would 13,602 km^3 and 3.602×10^{16} kg (3.602×10^{13} metric tons) respectively.

We note that these volume and mass estimates above are based on an assumed density contrast between the granite and host metasedimentary rocks of -150 kg m^{-3}. The density inferred from the *P*-wave velocity structure of Holder and Bott (1971) and the velocity/density relationships of Christensen and Mooney (1995) for the granite is 2648 kg m^{-3} which is consistent with the surface density measurements of Bott et al. (1958) and the density derived from cuttings in the 5 km deep Eden Geothermal EG-1 well in the St. Austell granite (Procyk, 2023). Bott et al. (1958), however, suggested that the surface density measurements might be in error by ±30 kg m^{-3}. Such an error would impact our volume and mass estimates. To test this, we decreased the density of the granite by 30 kg m^{-3} from 2648 to 2618 kg m^{-3} which increased the density contrast to -180 kg m^{-3} and then re-ran the three-dimensional model. We found that the volume and mass of the Cornubian granite corrected for root composition decreased from 76,367 km^3 and 2.022 $\times10^{17}$ kg (2.022×10^{14} metric tons) to 59,081 km^3 and 1.547×10^{17} kg (1.547×10^{14} metric tons) respectively, a reduction of some 23%. If we assume a similar percentage in the case that the density had, instead, been increased by 30 kg m^{-3} from 2648 to 2678 kg m^{-3} which decreased the density contrast to -120 kg m^{-3} then the volume and mass of the Cornubian granite corrected for root composition would increase from 76,367 km^3 and 2.022×10^{17} kg (2.022×10^{14} metric tons) to 93,653 km^3 and 2.508×10^{17} kg (2.508×10^{14} metric tons). These considerations suggest the volume estimate for the Cornubian granite has a most likely value of 76,367 km^3 and a minimum and maximum possible range of 59,081 to 93,653 km^3.

Irrespective, our volume estimates for the Cornubian batholith are significantly larger than the previous estimates (~40,000 km^3) of Williamson et al. (2010) based on the gravity models of Taylor (2007) and are of the order of estimates of Willis-Richards and Jackson (1989) based on the geophysical work of Bott et al. (1958) and others (~68,000 km^3).

Crustal Structure, Regional Gravity Anomalies, Topography, And The State of Isostasy

The emplacement of such large volumes of granite at high levels in the crust should have a profound effect on its structure, topography and bathymetry, and gravity anomaly. To investigate this further, we plot in Figure 14 the depth to the top and bottom of the modelled granite, together with the bathymetry and topography, regional Bouguer gravity anomaly and seismically constrained crustal structure along the Cornubian batholith axis. The profile, which is located in Figure 10b,c,d, extends from southwest of the Scilly Isles to northeast of Dartmoor and intersects (within 500 m either side of the profile) the Scilly Isles, Land's End, St. Austell and Dartmoor granite outcrops.

Figure 14 shows a strong correlation between the thickness of the modelled granite (pink shaded region) and the regional bathymetry and topography and Bouguer gravity anomaly: granite thickness decreases from northeast to southwest with a decrease in regional bathymetry and topography and with an increase in the regional Bouguer gravity anomaly. The thickest granite is associated with the most elevated topography and lowest regional gravity and the thinnest granite is associated with shallowest bathymetry and the highest regional gravity. We attribute the increase in regional Bouguer gravity anomaly to thinning of the crust towards the SouthWest Approaches. However, Moho depth appears to be constant at ~26.3 km (Pinet et al., 1991) along the BIRPS WAM line, which extends west of the Scilly Isles (Figure 10b) to the Goban Spur rifted margin, suggesting the thinning is unrelated to the present-day Atlantic rifted margin (Bullock and Minshull, 2005). An alternate possibility is that the crustal thinning occurred at the time of rifting of the Rheic Ocean northern volcanic margin during the Early Devonian to Late Carboniferous (Shail and Leveridge, 2009), but this does not explain the thinning of the granites along the axis of the batholith since it had a NNW-SSE extension vector. The most likely possibility therefore is Triassic rifting (ENE-WSW extension vector). Many of the NW-SE to NNW-SSE faults cutting Cornwall and south Devon were extensional faults during this episode (e.g., Shail and Alexander, 1997).

Irrespective, the close correlation observed in Figure 14b,c between the thickest granite and the most elevated topography suggests a link between them. We therefore follow Bott et al. (1958) who considered an Airy-Heiskanen model of isostasy in which the low-density granites acted as a supporting root (or compensation) to the surface topography. In this model, equilibrium is reached when the upward force due to low-density granite matches the downward force due to the high-density topography that has been created. To test this, we calculated the mass deficiency associated with the modelled granite (which was assumed to comprise both the batholiths and their underlying roots) and compared it to the mass excess associated with the topography of Cornwall and south Devon. In the case of the Cornubian batholith, the most likely volume is 76,367 $km^3 \times 10^9$ m^3 and the density contrast between the granites and the host metasedimentary rocks is -150 kg m^{-3}. This gives -1.145×10^{16} kg for the mass deficiency. In the case of the topography, the volume is 4525.8×10^9 m^3 and the density is the contrast with the surroundings (in this case air) = +2648 kg m^{-3}. This gives $+1.198 \times 10^{16}$ kg for the mass excess. These calculations show that the granites and topography are now very close to isostatic equilibrium.

The final question concerns the depth of compensation. An Airy-Heiskanen isostatic model places the depth of compensation at the Moho, usually at the base of the deepest root to the topography. However, Bott et al. (1958) suggested the compensation of Cornwall and south Devon was within the crust and at an unusually shallow depth of 10 or 15 km. The solid green lines in Figure 14 show the compensation depth computed assuming an Airy-Heiskanen model with a zero-elevation granite thickness of 10 km and a density of the granite and the underlying crust of 2648 and 3026 kg m^{-3} respectively. There is some evidence in Figure 14 of a correlation between the observed undulations of the base of the modelled granite body and the calculated root based on an Airy-Heiskanen model of local isostasy which supports the Bott model.

It is important to point out that the state of isostasy discussed above is based on an assessment of the present-day granite structure, topography, and gravity anomalies. However, we believe that because the crust (and lithosphere) is essentially elastic and is capable of supporting stresses on long geological timescales it has a 'memory' (e.g., Watts, 2023) and so observations made at Earth's surface at the present-day can be used to infer past geological events such as those associated with granite emplacement.

Stress

As several studies have pointed, local models of isostasy such as Airy-Heiskanen do not necessarily imply the crust is unable to support stress differences (e.g., Bott and Dean, 1972; Lambeck, 1980). For example, Bott and Dean (1972) showed using finite difference models that a rifted continental margin in Airy-Heiskanen isostatic equilibrium is associated with differential stresses caused by the load at the top of the crust and an equal and opposite upthrust near its base. They found a maximum stress difference of 37 MPa at a depth of ~10 km where the continental crust is 'squeezed' vertically compared to oceanic crust. It is not clear, however, whether such stresses could be supported by the strength of the crust without some form of yielding.

Some insight into the stresses involved in granite emplacement can be gained by consideration of a prism of unit area floating on a substratum that is subject to vertical shear stresses generated, for example, by locally applied loads or flexural bending. A downward stress would result in a mass deficiency while an upward stress would result in a mass excess. Gunn (1943) showed that:

$$S_v = Mg$$

where S_v is a vertical shear stress, M is the mass/per unit area of the displaced material and g is average gravity. If we assume $g = 9.8$ m s^{-2} and that the displaced material is given by the topography in Cornwall and south Devon which has a mass of 1.198×10^{16} kg and an area of 4.79×10^{10} m^2 then, the S_v, the shear stress associated with granite emplacement is 2.5 MPa. This is a modest stress and sufficient, most probably, to be supported by the strength of the crust which explains why the individual plutons that comprise the Cornubian batholith, together with their associated gravity anomalies, have been maintained for such long periods of geological time.

Granite Emplacement

As shown by Bott and Smithson (1967), gravity anomalies can be used to constrain granite emplacement mechanisms and whether they formed, for example, by forcible intrusion, stoping of host rocks, cauldron subsidence or some combination of these processes. Forcible intrusion is associated with a gravity anomaly that resembles observations but implies shouldering and uplift of surrounding host rocks. Stoping, in which relatively dense host rocks break off and sink through the rising granite magma, produces a gravity 'high' which flattens the 'low' over the granite. If, however, the stoped material sinks to the base of the crust and then loads it, the effect of the high is reduced because of floor subsidence. Bott argued that such a model also produces a gravity anomaly that is in accord with observations.

The gravity models used to construct Figures 12-14 differ from those of Bott and colleagues in that they do not assume a priori a flat base to the granite. We have shown that models of an outward sloping batholith which comprise several plutons underlain by a root are also in accord with observations (e.g., Figure 11a,b). Although other explanations are possible (e.g., the floor subsidence model of Cruden and McCaffrey, 2001), we believe the root to be a frozen melt/mush zone which was once part of a feeder system that channelled granite magma from the middle crust to higher crustal levels. Figure 14 shows that the base of the granite batholith dips gently to the northeast from ~11 km beneath Land's End to ~12 km beneath Dartmoor while the roots protrude locally into the middle crust to depths of ~14 km beneath the Cligga Head and Carnmenellis plutons, ~12.5 km beneath the St. Austell pluton and >15 km beneath the Dartmoor pluton. The seismic reflectors (Figure 14) are problematic in that they do not all correspond closely to major crustal boundaries. The R1 reflector, for example, appears within the gravity modelled batholith which is difficult to explain given the expected homogeneous nature of the granite in depth. The R2 and R3 reflectors beneath Cligga Head, Hingston Down and Kit Hill and Dartmoor plutons, however, do correspond to the modelled lower boundary of the granite and the Moho respectively. The main exception is the R3 reflector beneath Dartmoor, which is deeper than expected and may, we speculate, indicate the base of an alkaline magmatic underplate which forms the source of the lamprophyre dykes which are coeval with granite emplacement (Dupuis et al., 2015).

Figure 15 shows a summary geological model at true-scale (i.e., vertical = horizontal scale) profile along the batholith axis. The pink shaded area shows the granite inferred from the gravity model in Figure 14. The brown solid lines schematically show an interpretation of the shape of individual plutons that comprise the batholith. The interpretation has been guided by sampling the second horizontal derivative of the Bouguer gravity anomaly, which is sensitive to the slopes of a granite pluton (e.g., Figures 6-7), along the batholith axis. The actual structure along the base of the granite (blue line) remains, however, uncertain. We speculated earlier that the Cornubian and probably Haig Fras granites are most likely derived from amphibolite facies metasediments in the middle crust. The lower part of the pink shaded area could be a migmatite terrane (partly leucosome melt, part metamorphic restite), as seen for example along the Himalaya.

Seismic data (Holder and Bott, 1971; Brooks et al., 1984) suggest the granitic upper crust extends to depths ~10-11 km and the reflective lower crust identified on the BIRPS

SWAT 4 and WAM seismic reflection lines extends from a depth of ~20 km to Moho at ~27 km. Therefore, the middle crust comprises a ~9-10 km thicker layer which we believe is the source of the granite magmas. Specifically, the granites are considered to have been derived from muscovite or biotite dehydration reactions at temperatures of ~700 to ~800ºC and low pressures (~300 to ~600 MPa) from a dominantly pelitic or psammitic melt source in the middle crust (e.g., Simons et al., 2016; Searle et al., Part 1). The middle crust layer is underlain by the reflective lower crust which is believed to comprise dry granulite facies rocks (Searle et al., Part 1). The source of heating of the middle crust therefore remains unclear, although it might be related to sill and dyke intrusions in the reflective lower crust, magmatic underplating, or some form of temperature anomaly in the sub-crustal mantle.

Isostatic considerations are consistent with a granitic source in the middle crust. As was noted earlier Cornwall and south Devon appear to be approximately in isostatic equilibrium with a balance existing between the mass deficiency of the granites and the mass excess of the topography. The balance supports the view (Searle et al., Part 1) of upward flaring conduits feeding individual plutons in the upper crust that bulge the surface upwards because of magmatic injection and roof inflation. Such a model is therefore a ‘hybrid’ which has elements of both the batholith model of Bott et al. (1958) and the sill model of Taylor, (2007). Furthermore, the presence of an isostatic compensation depth that is within the crust (rather than at the Moho) and at the base of the batholith is consistent with data from experimental rock mechanics (Kohlstedt et al., 1995). For temperatures of 400 to 800ºC, for example, deformation would be plastic and controlled by glide of dislocations rather than by thermally activated creep. In this case, the middle crust would have acted as a mechanically weak zone during granite emplacement, effectively decoupling the topography from any support it might otherwise have received from the lower crust and/or upper mantle.

CONCLUSIONS

- A newly compiled Bouguer gravity anomaly 250 × 250 m grid has been used along with two- and three-dimensional forward and inverse gravity modelling to constrain the structure of the Cornubian batholith of SW England.

- Gravity modelling suggests the Cornubian batholith comprises several individual plutons which slope outwards in their upper part and extends to depths of up to 10-11 km.

- The steepest slopes bound the Land's End, St. Austell, Bodmin and Dartmoor plutons where they appear to align along Variscan trends.

- Individual granite plutons are underlain by roots which protrude downwards into the middle crust.

- Cornwall and south Devon appear to be close to a state of isostatic equilibrium in which the mass deficiency of the low-density granites is in approximate balance with the mass excess of the high-density topography.

- The most likely depth of compensation is in the middle crust which is consistent with both temperature considerations for the derivation of granite magmas and with low-temperature plastic flow laws.

- Isostatic considerations are consistent with a model of upward flaring conduits feeding individual plutons that bulge the surface upwards because of magmatic injection and roof inflation. Such a model may be viewed as a ‘hybrid’ which has elements of both the batholith and sill granite emplacement models.

- The Haig Fras batholith may also comprise individual plutons, but there is no evidence of any connection between these offshore granites and the onshore Cornubian granites.

- The volume and mass of the Cornubian granites is estimated at 76,367 km^3 and 2.022×10^{17} kg (2.022×10^{14} metric tons) respectively, assuming a density contrast between granite and host metasediment of -150 kg m^{-3}, a granite density of 2648 kg m^{-3} and roots that comprise and an equal proportion of granite and migmatite. These estimates will vary, depending on actual root composition, density contrast and granite density.

Acknowledgements

The gravity, bathymetry and topography data used in this paper are available from the British Geological Survey (https://www.bgs.ac.uk/datasets/gb-land-gravity-survey), the European Marine Observation and Data Network (https://emodnet.ec.europa.eu/en/bathymetry) and the Scripps Institution of Oceanography (https://topex.ucsd.edu/cgi-bin/get_data.cgi). Figures were constructed using GMT (Wessel and Luis, 2017) and Affinity Designer.

References Cited

Al-Kindi, S., White, N., Sinha, M., England, R., and Tiley, R., 2002, Crustal trace of a hot convective sheet: Geology, p. 207-210, https://doi.org/10.1130/0091-7613(2003)031<0207:CTOAHC>2.0.CO;2

Al-Rawi, F. R. J., 1980, A geophysical study of deep structures in southwest Britain. [Ph.D: University of Wales].

Alexander, A. C., Shail, R. K., and Leveridge, B. E., 2019, Late Paleozoic extensional reactivation of the Rheic–Rhenohercynian suture zone in SW England, the English Channel and Western Approaches, *in* Wilson, R. W., Houseman, G. A., McCaffrey, K. J. W., Dore, A. G., and Buiter, S. J. H., eds., Fifty Years of the Wilson Cycle Concept in Plate Tectonics, Volume 470, Geological Society, London, Special Publications, p. 353-373, https://doi.org/10.1144/SP470.19

Bassett, D., and Watts, A. B., 2015, Gravity anomalies, crustal structure, and seismicity at subduction zones: 1. Seafloor roughness and subducting relief: Geochemistry Geophysics Geosystems, v. 16, https://doi.org/10.1002/2014GC005684

BIRPS, 1986, Deep seismic reflection profiling between England, France and Ireland: J. Geol Soc. London, v. 143, p. 45-52, https://doi.org/10.1144/gsjgs.143.1.0045

Bott, M. H. P., 1960, The use of Rapid Digital Computing Methods for Direct Gravity Interpretation of Sedimentary Basins: Geophys. J. R. astr. Soc., v. 3, p. 63-67, https://doi.org/10.1111/j.1365-246X.1960.tb00065.x

Bott, M. H. P., 1962, A simple criterion for interpreting negative gravity anomalies: Geophysics, v. 27, p. 376-381, https://doi.org/10.1190/1.1439026

Bott, M. H. P., Day, A. A., and Masson-Smith, D., 1958, The geological interpretation of gravity and magnetic surveys in Devon and Cornwall: Phil. Trans. Roy. Soc., v. 215A, p. 161-191, https://doi.org/10.1098/rsta.1958.0013

Bott, M. H. P., and Dean, D. S., 1972, Stress Systems at Young Continental Margins: Nature, v. 235, p. 23-25, https://doi.org/10.1038/physci235023a0

Bott, M. H. P., and Scott, P., 1964, Recent geophysical studies in south-west England, *in* Hosking, K. F. G., and Shrimpton, G. J., eds., Present View of some Aspects of the Geology of Cornwall: Truro, Royal Geological Society of Cornwall, p. 25-44.

Bott, M. H. P., and Smithson, S. B., 1967, Gravity investigations of subsurface shape and mass distributions of granite batholiths: Geol. Soc. Am. Bull, v. 78, p. 859-878, https://doi.org/10.1130/0016-7606(1967)78[859:GIOSSA]2.0.CO;2

Brooks, M., Doody, J. J., and Al-Rawi, F. R. J., 1984, Major crustal reflectors beneath SW England: J. Geol Soc. London, v. 141, p. 97-103, https://doi.org/10.1144/gsjgs.141.1.0097

Bullock, A. D., and Minshull, T. A., 2005, From continental extension to seafloor spreading: crustal structure of the Goban Spur rifted margin, southwest of the UK: Geophys. J. Int, v. 163, p. 527-546, https://doi.org/510.1111/j.1365-1246X.2005.02726.x.

Chappell, R., and Hine, R., 2006, The Cornubian Batholith: an example of magmatic fractionation on a crustal scale: Resource Geology, v. 56, p. 203-244, https://doi.org/10.1111/j.1751-3928.2006.tb00281.x

Chen, Y., Clark, A. H., Farrar, E., Wasteneys, H., Hodgson, M. J., and Bromley, A. V., 1993, Diachronous and independent histories of plutonism and mineralization in the Cornubian batholith: Journ. Geol. Soc., v. 150, p. 1183-1191, https://doi.org/10.1144/gsjgs.150.6.1183

Chesley, J. T., Halliday, A. N., Snee, L. W., Mezger, K., Shepherd, T., and Scrivener, R. C., 1993, Thermochronology of the Cornubian batholith in SW England: Implication for pluton emplacement and protracted hydrothermal mineralization: Geochimica et

Cosmochimica Acta, v. 57, p. 1817-1835, https://doi.org/10.1016/0016-7037(93)90115-D

Christensen, N. I., and Mooney, W. D., 1995, Seismic velocity structure and composition of the continental crust: A global view: J. Geophys. Res., v. 100, p. 9761-9788, https://doi.org/10.1029/95JB00259

Cruden, A. R., and McCaffrey, K. J. W., 2001, Growth of plutons by floor subsidence: implications for rates of emplacement, intrusion spacing and melt-extraction mechanisms: Physics and Chemistry of the Earth, Part A: Solid Earth and Geodesy, v. 26, no. 4-5, p. 303-315, https://doi.org/10.1016/S1464-1895(01)00060-6

Cordell, L., and Henderson, R. G., 1968, Iterative three-dimensional solution of gravity anomaly data using a digital computer: GEOPHYSICS, v. 33, p. 596-601, https://doi.org/10.1190/1.1439955

De La Beche, H. T., 1839, Report on the Geology of Cornwall, Devon and West Somerset: With 12 Plates, H.M. Stationery Office - Cornwall (England), Longman, 648 pp.

Dupuis, N. E., Braid, J. A., Murphy, J. B., Shail, R. K., Archibald, D. A., and Nance, R. D., 2015, 40Ar/39Ar phlogopite geochronology of lamprophyre dykes in Cornwall, UK: new age constraints on Early Permian post-collisional magmatism in the Rhenohercynian Zone, SW England: Journ. Geol. Soc., v. 172, p. 566-575, https://doi.org/10.1144/jgs2014-151

Edwards, J. W. F., 1984, Interpretations of seismic and gravity surveys over the eastern part of the Cornubian platform, *in* Hutton, D. H. W., and Sanderson, D. J., eds., Variscan Tectonics of the North Atlantic Region, Volume Special Publication 14: London, Geol. Soc. London, p. 119-124, https://doi.org/10.1144/GSL.SP.1984.014.01.11

Exley, C. S., 1966, The granitic rocks of Haig Fras: Nature, v. 210, p. 365-367, https://doi.org/10.1038/210365a0

Exley, C. S., and Stone, M., 1982, Hercynian intrusive rocks, *in* Sutherland, D. S., ed., Igneous Rocks of the British Isles, p. 287-320.

Evans, C. D. R., 1990, The geology of the western English Channel and its western approaches, London, HMSO, United Kingdom Offshore Report, 93 pp.

Farndale, H., and Law, R., An Update on the United Downs Geothermal Power Project, Cornwall, UK, *in* Proceedings Workshop on Geothermal Resevoir Engineering, Stanford University, Stanford, California, February 7-9, 2022, Volume SGP-TR-223, p. 1-13.

Floyd, P. A., Exley, C. S., and Styles, M. T., 1993, The Igneous Rocks of SW England, London, Chapman and Hall, 256 pp.

Götze, H. J., and Lahmeyer, B., 1988, Application of three-dimensional interactive modeling in gravity and magnetics: Geophysics, v. 53, p. 1096-1108, https://doi.org/10.1190/1.1442546

Gunn, R., 1943, A quantitative evaluation of the influence of the lithosphere on the anomalies of gravity: Franklin Inst. J., v. 236, p. 47-65, https://doi.org/10.1016/S0016-0032(43)91198-6

Henes, P., Shail, R., Dalby, C., Rollinson, G., Broom-Fendley, S., and Andersen, J., 2023, Mineralogical, mineral chemical and whole-rock geochemical variation in the upper 4.5 km of the Cornubian batholith - initial 3D glimpses from the Eden Geothermal Project.

Holder, A. P., and Bott, M. H. P., 1971, Crustal structure in the vicinity of South-west England: Geophys. J. R. astr. Soc., v. 23, p. 465-489, https://doi.org/10.1111/j.1365-246X.1971.tb01838.x

Hughes, S. P., Stickland, R. J., Shail, R. K., LeBoutillier, N. G., Alexander, A., and Thomas, M., 2009, The chronology and kinematics of Late Palaeozoic deformation in the NW contact metamorphic aureole of the Land's End Granite.: Geoscience in South-west England, v. 12, p. 140-152.

Jones, D. G., Miller, J. M., and Roberts, P. D., 1988, A seabed radiometric survey of Haig Fras, S. Celtic Sea, U.K.: Proc. Geol. Assoc., v. 99, p. 193-203, https://doi.org/10.1016/S0016-7878(88)80035-X

Klemperer, S., and Hobbs, R., 1991, The BIRPS Atlas: Deep seismic reflection profiles around the British Isles: Cambridge, Cambridge University Press, 124 pp.

Kohlstedt, D. L., Evans, B., and Mackwell, S. J., 1995, Strength of the lithosphere: Constraints imposed by laboratory experiments: J. Geophys. Res., v. 100, p. 17587-17602, https://doi.org/10.1029/95JB01460

Lambeck, K., 1980, Estimates of stress differences from isostatic considerations: J. Geophys. Res., v. 85, p. 6397-6402, https://doi.org/10.1029/JB085iB11p06397

Laving, G. J., 1971, Automatic methods for the interpretation of gravity and magnetic field anomalies and their application to marine geophysical surveys, [Ph.D University of Durham], 152 p.

Meissner, R., 1986, Twenty years of deep seismic reflection profiling in Germany - a contribution to our knowledge of the nature of the lower Variscan crust: J. Geological Soc. London Special Publication No. 24, p. 1-10, https://doi.org/10.1144/GSL.SP.1986.024.01.02

Müller, A., Seltmann, R., Halls, C., Siebel, W., Dulski, P., Jeffries, T., Spratt, J., and Kronz, A., 2006, The magmatic evolution of the Land's End pluton, Cornwall, and associated pre-enrichment of metals: Ore Geology Reviews, v. 28, p. 329-367, https://doi.org/10.1016/j.oregeorev.2005.05.002

Pinet, B., Sibuet, J.-C., Lefort, J.-P., Schroeder, I., and Montadert, L., 1991, Structure profonde de Ia marge des entrées de la Manche et du plateau continental celtique: Ie profil WAM: Mém. Soc. géol. France, v. 159, p. 167-183.

Prive, E., 1986, Seismic interpretation and gravity modelling of BIRPS SWAT Lines 5 and 6: British Geological Survey, Marine Report 87/14, 3 pp + 3 Figures.

Procyk, A., 2023, UK's longest geothermal well heats biomes, https://www.ogj.com/energy-transition/article/14298718/uks-longest-geothermal-well-heats-biodomes.

Reinecker, J., Gutmanis, J., Foxford, A., Cotton, L., Dalby, C., and Law, R., 2021, Geothermal exploration and reservoir modelling of the United Downs deep geothermal project, Cornwall (UK): Geothermics, v. 97, https://doi.org/10.1016/j.geothermics.2021.102226

Sandwell, D. T., Harper, H., Tozer, B., and Smith, W. H. F., 2019, Gravity field recovery from geodetic altimeter missions: Advances in Space Research, https://doi.org/10.1016/j.asr.2019.09.011

Schmidt, S., Götze, H. J., Fichler, C., and Alvers, M., 2010, IGMAS+ – a new 3D gravity, FTG and magnetic modeling software, *in* Zipf, A., Behncke, K., Hillen, F., and Scheffermeyer, J., eds., GEO-INFORMATIK Die Welt im Netz: Heidelberg, Germany, Akademische Verlagsgesellschaft AKA GmbH, p. 57-63.

Searle, M. P., Shail, R., Pownall, J., Jurkowski, C., Watts, A. B., and Robb, L., The Permian Cornubian granites of SW England; Part 1: Field, structural and petrological constraints, Submitted

Shail, R. K., and Alexander, A. C., 1997, Late Carboniferous to Triassic reactivation of Variscan basement in the western English Channel: Evidence from onshore exposures in south Cornwall: J. Geol Soc. London, v. 154, p. 163-168.

Shail, R. K., Stuart, F. M., and Wilkinson, J. J., 2003, The role of post-Variscan extensional tectonics and mantle melting in the generation of the Lower Permian granites and the giant W-As-Sn-Cu-Zn-Pb orefield of SW England: Applied Earth Science: Transactions of the Institutions of Mining and Metallurgy: section B, http://hdl.handle.net/10036/3644

Shail, R. K., and Leveridge, B. E., 2009, The Rhenohercynian passive margin of SW England: Development, inversion and extensional reactivation: Comptes rendus: Geoscience, v. 341, p. 140-155, https://doi.org/10.1016/j.crte.2008.11.002

Simons, B., Andersen, J. Ø., Shail, R. K., and Jenner, F. E., 2017, Fractionation of Li, Be, Ga, Nb, Ta, In, Sn, Sb, W, and Bi in the peraluminous Early Permian Variscan granites of the Cornubian batholith: Precursor processes to magmatic- hydrothermal mineralization: Lithos, v. 278-281, p. 491-512, https://doi.org/10.1016/j.lithos.2017.02.007

Simons, B., Shail, R. K., and Andersen, J. Ø., 2016, The petrogenesis of the Early Permian Variscan granites of the Cornubian Batholith: Lower plate post-collisional peraluminous magmatism in the Rhenohercynian zone of SW England: Lithos, v. 260, p. 76-94, https://doi.org/10.1016/j.lithos.2016.05.010

Smith, A. J., Stride, A. H., and Whittard, W. F., 1965, The geology of the Western Approaches of the English Channel IV A recently discovered Variscan granite west-north-west of the Scilly Isles: Colston Papers, v. 17, p. 287-301.

Smith, W. D., Darling, J. R., Bullen, D. S., Lasalle, S., Pereira, I., H.Moreira, Allen, C. J., and Tapster, S., 2019, Zircon perspectives on the age and origin of evolved S-type granites from the Cornubian batholith, Southwest Britain.: Lithos, v. 336-337, p. 14-26, https://doi.org/10.1016/j.lithos.2019.03.025

Stone, M., and Exley, C. S., 1985, High heat production granites of southwest England and their associated mineralization: a review: Transactions of the Institution of Mining and Metallurgy. Section B, Applied Earth Science, v. 95, p. B25-B36.

Talwani, M., and Ewing, M., 1960, Rapid Computation of Gravitational Attraction of Three-Dimensional Bodies of Arbitrary Shape: Geophysics, v. 25, no. 1, p. 205-223, https://doi.org/10.1190/1.1438687

Tanner, J. G., 1967, An automated method of gravity interpretation: Geophys. J., v. 13, p. 339-347, https://doi.org/10.1111/j.1365-246X.1967.tb02164.x

Taylor, G. K., 2007, Pluton shapes in the Cornubian batholith: new perspectives from gravity modelling: J. Geol. Soc. London, v. 164, p. 525-528, https://doi.org/10.1144/0016-76492006-104

Tombs, J. M. C., 1977, A study of the space form of the Cornubian granite batholith and its application to detailed gravity surveys in Cornwall, Report, Institute of Geological Sciences: London, Department of Industry, 5pp.

Warner, M., Spaargaren, B., Watts, D., and Doody, J., 1994, High resolution images of the lower crust: deep seismic reflections from15 to 180Hz: Tectonophysics, v. 232, p. 235-237, https://doi.org/10.1016/0040-1951(94)90086-8

Watts, A. B., 2023, Isostasy and Flexure of the Lithosphere, 2nd Edition, Cambridge University Press, 583 pp., https://doi.org/ 10.1017/9781139027748

Wessel, P., and Luis, J. F., 2017, The GMT/MATLAB Toolbox: Geochemistry Geophysics Geosystems, v. 18, p. 811-823, https://doi.org/10.1002/2016GC006723

Williams, G. D., and Chapman, T. J., 1986, The Bristol-Mendip foreland thrust belt: J. Geol. Soc. London, v. 143, p. 63-73, https://doi.org/10.1144/gsjgs.143.1.0063

Williamson, B. J., Müller, A., and Shail, R. K., 2010, Source and partitioning of B and Sn in the Cornubian batholith of southwest England: Ore Geology Reviews, v. 38, p. 1-8, https://doi.org/10.1016/j.oregeorev.2010.05.002

Willis-Richards, J., and Jackson, N. J., 1989, Evolution of the Cornubian Ore Field, Southwest England: Part I. Batholith Modeling and Ore Distribution: Economic Geology, v. 84, p. 1078-1100.

Figure Captions

Figure 1. Principal data sets used in this study. a) Bouguer gravity anomaly onshore and offshore (Black filled circles) derived from a BGS data onshore and satellite-derived gravity data offshore. LE = Land's End, C = Carnmenellis, CH = Cligga Head, SA = St. Austell, KH = Kit Hill, B = Bodmin and D = Dartmoor. b) Bathymetry data offshore and topography data onshore derived from a EMODnet and OpenStreetMap grid respectively.

Figure 2. Bouguer gravity anomaly maps of south-west England based on BGS data onshore and satellite-derived data offshore. a) Bouguer gravity anomaly. Contour interval = 10 mGal. Purple lines delineate the main Cornubian granites. D = Dartmoor, B = Bodmin Moor, SA = St. Austell, C = Carnmenellis, LE = Land's End, CH = Cligga Head, S = Scilly Isles and TG = Tregonning-Godolphin. Dashed grey line shows the seismic Line 1 of (Holder and Bott, 1971). Solid black lines show BIRPS lines SWAT 4, 5, 8 and 9 (Klemperer and Hobbs, 1991). b) regional background field as derived from a median filter (w = 300 km) of the observed Bouguer gravity anomaly. Contour interval = 2.5 mGal. c) Residual Bouguer gravity anomaly as derived by subtraction of the median filter from the observed Bouguer gravity anomaly.

Figure 3. Ensemble averages of observed Bouguer gravity anomaly profiles 1-8 (Figure 2c). Black lines show the individual profiles and red lines show the ensemble average. Note the ensemble average retains features in the observed anomaly that are common to each profile such as the slight asymmetry of the gravity 'low' and the small amplitude flanking 'high' while at the same time suppresses features that only appear on a few of the profiles.

Figure 4. Interpretation of the ensemble profile (red curve in Figure 3) in terms of an outward sloping granite body which has a density contrast with its surrounding of -150 kg m^{-3} and a flat base. The main granite body has a width at its base of ~40 km and a depth below sea-level of ~10 km. Also shown are the blocks of surface mass assumed in the inversion, the point of intersection on the profile of the granite outcrops and the Holder and Bott (1971) seismic line, and the difference between the observed and calculated gravity anomaly.

Figure 5. The granite body (light purple shading) determined in Figure 4 in the context of the seismic structure of the region derived by Holder and Bott (1971) and Brooks et al., (1984). The depth to the base of the granite batholith of ~10 km is generally consistent with the wide-angle refraction and reflection results of Holder and Bott (1971) and Brooks et al., (1984). R1 = reflection from within the granite body. R2 = probable reflection from the base of the granite. R3 = reflection from the Moho. Dark purple shading delineates a hypothetical root to the batholith interpreted here as protruding into the middle crust which is interpreted by Searle et al. Part 1 as comprising amphibolite facies rocks. The thick horizontal lines schematically illustrate the reflective layered lower continental crust as seen on BIRPS SWAT 9 (Alexander et al., 2019) and WAM (Pinet et al., 1991) seismic profiles and

interpreted by Searle et al. Part 1 as granulite facies rocks. The observed and calculated Bouguer gravity anomaly is compared to the gravity effect of the root.

Figure 6. A simple model for the gravity anomaly and second horizontal derivative associated with an outward sloping body which has a uniform density contrast with its surroundings of -150 kg m^{-3}.

Figure 7. Second horizontal derivative of the Bouguer gravity anomaly map of SW England. Note that the Dartmoor, Bodmin, St. Austell, Carnmenellis and Land's End granites are associated with positive second horizontal derivatives within the outcrop region (yellow filled dots) suggesting the sub-surface slope of the granite slopes outwards. The Dartmoor and Bodmin granites are associated with a flanking negative. The most intense derivatives, indicative of the steepest slopes, have a distinct east-west, Variscan, trend.

Figure 8. Interpretation of an ensemble averaged profile of the Carnmenellis granite showing the effect on the structure of different assumed density contrasts. a) Location map showing the profiles used to construct the ensemble average. Filled green triangle locates South Crofty mine. Solid grey line shows the location of the profile modelled in Figure 9. b) Observed and calculated Bouguer gravity and Residual anomaly for Model 2 which assumes a density contrast of -150 kg m^{-3}.

Figure 9. Interpretation of a Bouguer gravity anomaly profile across the Carnmenellis granite. The profile (Figure 8a), which intersects the South Crofty mine at distance 49.1 km, shows the effect of dimensionality on the structure of the granite. Pink shaded region shows the two-dimensional structure. Dashed blue lines show the effect of three-dimensionality.

Both cases of dimensionality assume a density contrast of -200 kg m^{-3}. The calculated Bouguer gravity and Residual anomaly are based on the two-dimensional case.

Figure 10. Bathymetry/topography and Bouguer gravity anomaly of the enlarged area. a) Residual Bouguer gravity anomaly obtained by subtracting the regional field from the observed Bouguer gravity anomaly. Thin black lines show the 79 'sections' along which the residual anomaly is modelled. Thick white lines locate sections comparing observed and calculated gravity anomalies shown in Figure 11a,b. b) Regional background field obtained by median filtering the observed Bouguer gravity anomaly (*w* = 300 km). Contour interval = 2.5 mGal. c) Observed Bouguer gravity anomaly. HFSB = Haig Fras Sub-Basin. SWAB = South-west Approaches Basin. CSB = Celtic Sea Basin. Thin white lines locate the BIRPS SWAT5, SWAT6 and WAM seismic reflection profiles and the 'dip-line' reflection profiles of Brooks et al. (1984). d) Bathymetry/topography based on a EMODnet and OpenStreetMap grid. Thick white line locates the batholith axis profile in Figure 13.

Figure 11a. Comparison of the observed and calculated Bouguer gravity anomaly along vertical sections 11, 14, 30 and 38 of the onshore granites. Grey line is the observed Bouguer gravity anomaly. Red line is the calculated. Blue is the residual obtained by subtracting the calculated Bouguer anomaly from the observed anomaly. Red dashed line is the gravity effect of the root. Upper black dashed line is mean sea-level. Lower black dashed line is the 10 km depth. Profiles are stacked on the maximum depth of the root (thick dashed grey line).

Figure 11b. Comparison of the observed and calculated Bouguer gravity anomaly along vertical sections 40, 45, 47 and 73 of the offshore granites.

Figure 12. Perspective views of the Cornubia and Haig Fras granite bodies from three-dimensional gravity modelling. Light blue delineates the known outcrop of granite in Cornubia and the region of possible granites at Haig Fras. a) View looking northeast from azimuth 220^{o} and elevation 10^{o}. b) View looking south-west from azimuth 040^{o} and elevation 10^{o}.

Figure 13. Map view showing the relationship between the outer limit of the Cornubian and Haig Fras granites and the coastline of Cornwall and south Devon, the outcrop of the main plutons, and the topography and bathymetry. a) Granite thickness derived from the difference between the base (including the root) and top of the granite. Symbols as in Figure 1. b) Outer limit of granite and its relationship to the coast and topography and bathymetry.

Figure 14. Comparison of the depth to the top and bottom of the modelled Cornubian granite batholith to the bathymetry and topography and regional Bouguer gravity field along the batholith axis (Figure 10b,c,d) from southwest of the Scilly Isles to Dartmoor. a) regional Bouguer anomaly used to separate the gravity anomaly associated with the granites from the regional background field. b) Bathymetry (offshore) and topography (onshore). Purple filled triangles and grey shaded regions indicate granite outcrop. c) Crustal model along the batholith axis. P-wave velocities are based on Holder and Bott (1971) and densities have been derived from the empirical velocity/density relationships of Christensen and Mooney (1995). Solid black lines showing deep geothermal wells, UD-1 (Reinecker et al., 2021; Farndale and Law, 2022) and EG-1 (Procyk, 2023) in the batholith. Thin dashed black lines show the seismically constrained depths to the base of the granite and the Moho. Dark grey dashed lines show Reflectors R1, R2 and R3 of Brooks et al. (1984). Red filled triangles show the top of the modelled granite along each of the 79 vertical sections. Blue filled triangles show

the base of the granite. Dashed purple line shows the predicted Moho based on the regional Bouguer anomaly in a) and the thin black dashed line the seismically predicted Moho of Holder and Bott (1971). Green solid lines show the predicted "root' based on bathymetry and topography and its Airy-type compensation at a depth of 10 km in the crust.

Figure 15. Crustal model along the batholith axis at true scale showing, schematically, the outlines of individual plutons that comprise the Cornubian batholith. a) The second horizontal derivative of the Bouguer gravity anomaly (Figure 6) the steep slopes of which are used to estimate the edges of the individual plutons. b) Crustal model at true vertical scale showing the edges of the main plutons (solid brown lines). Dashed brown lines show uncertain edges. Vertical purple lines locate the UD-1 and EG-1 (Figure 13). The depth of amphibolite and granulite facies rocks is schematic.

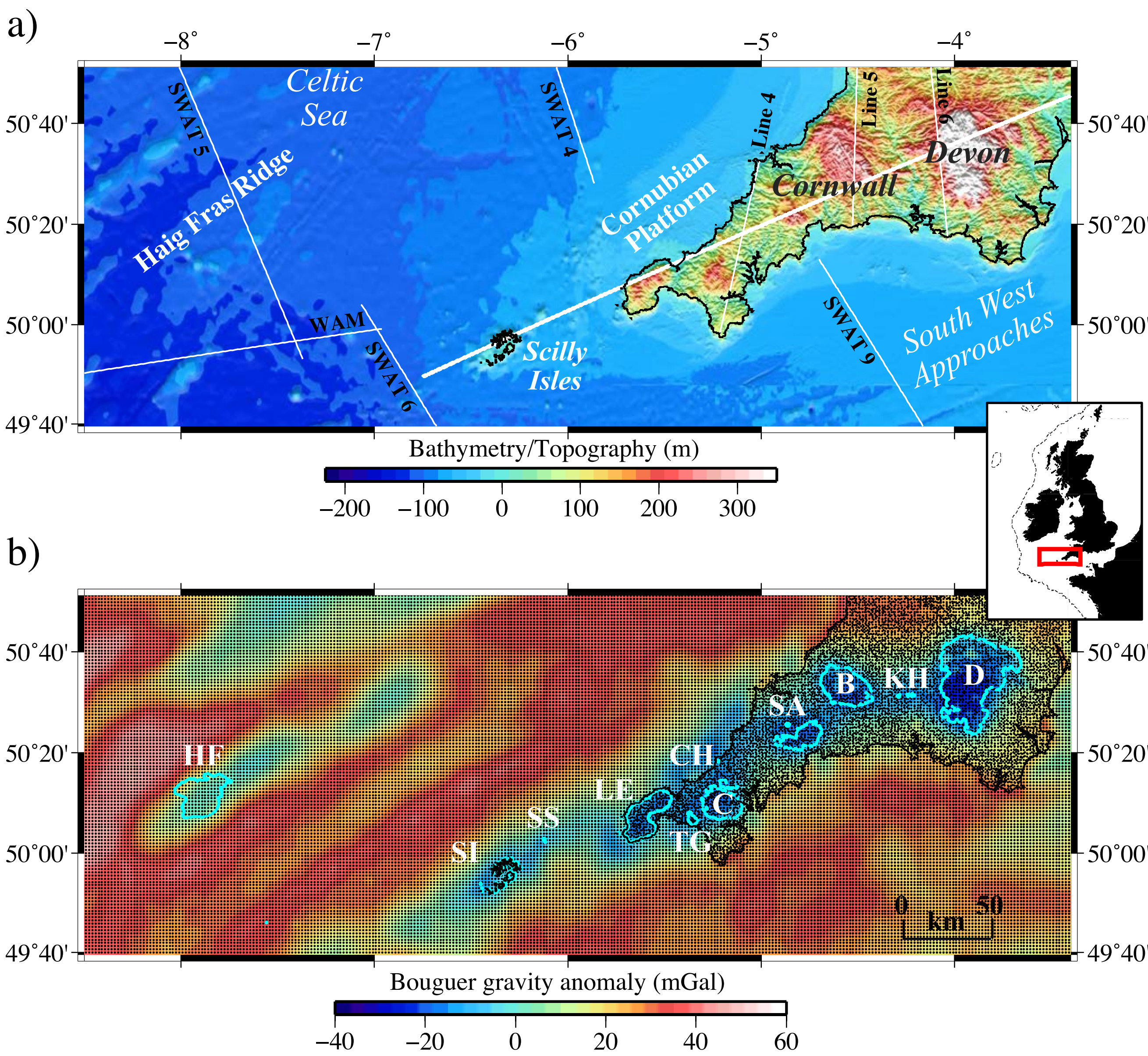

a)
b)
−8°
−7°
−6°
−5°
−4°
50°40'
50°20'
50°00'
49°40'
Celtic Sea
Haig Fras Ridge
SWAT 5
SWAT 4
SWAT 6
SWAT 9
WAM
Line 4
Line 5
Line 6
Cornubian Platform
Cornwall
Devon
Scilly Isles
South West Approaches
Bathymetry/Topography (m)
−200
−100
0
100
200
300
HF
SI
SS
LE
CH
TG
C
SA
B
KH
D
0 50
km
Bouguer gravity anomaly (mGal)
−40
−20
0
20
40
60

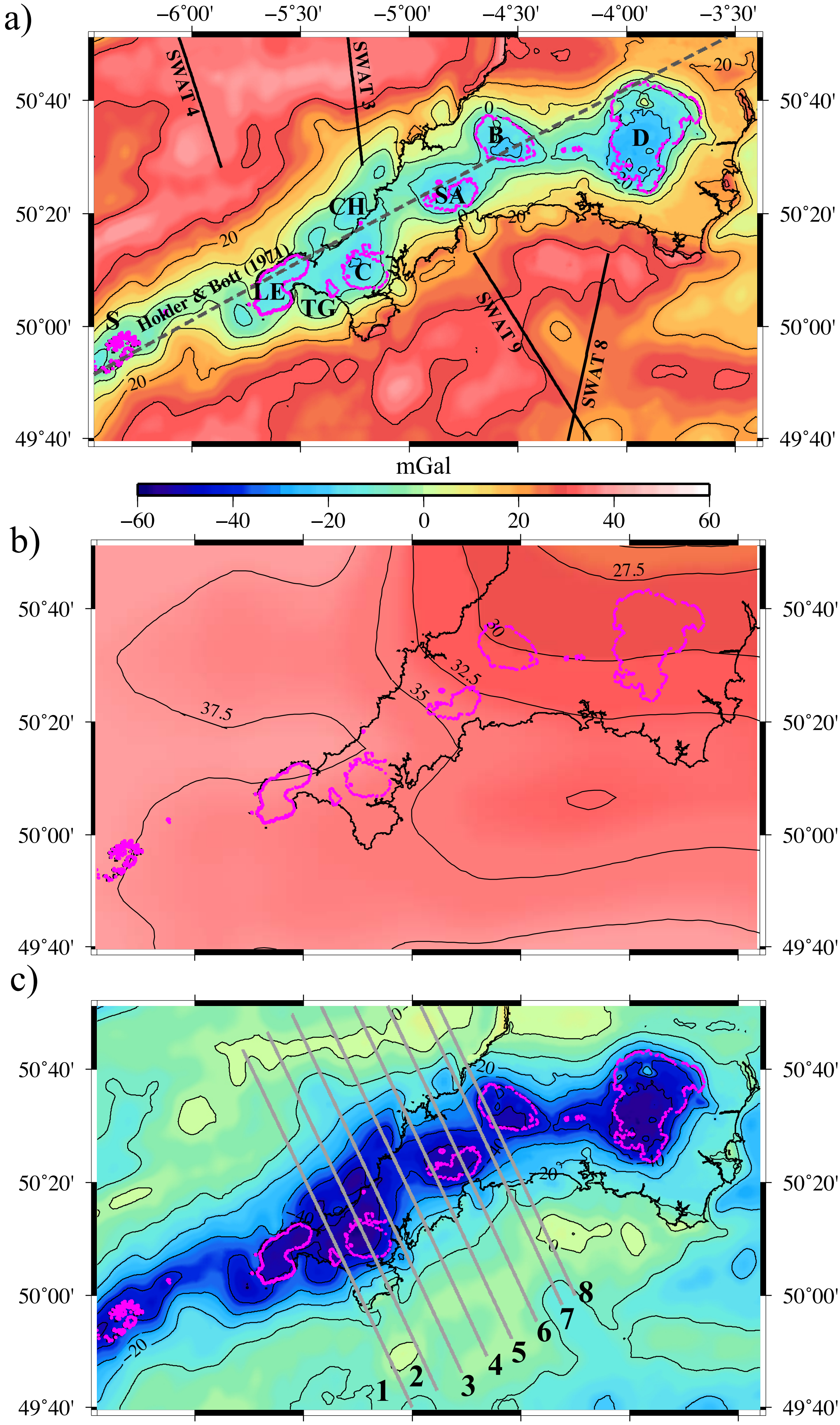
a)
−6°00'
−5°30'
−5°00'
−4°30'
−4°00'
−3°30'
50°40'
50°20'
50°00'
49°40'
SWAT 4
SWAT 3
SWAT 9
SWAT 8
Holder & Bott (1971)
S
LE
TG
CH
C
SA
B
D
mGal
−60
−40
−20
0
20
40
60
b)
27.5
30
32.5
35
37.5
c)
1
2
3
4
5
6
7
8

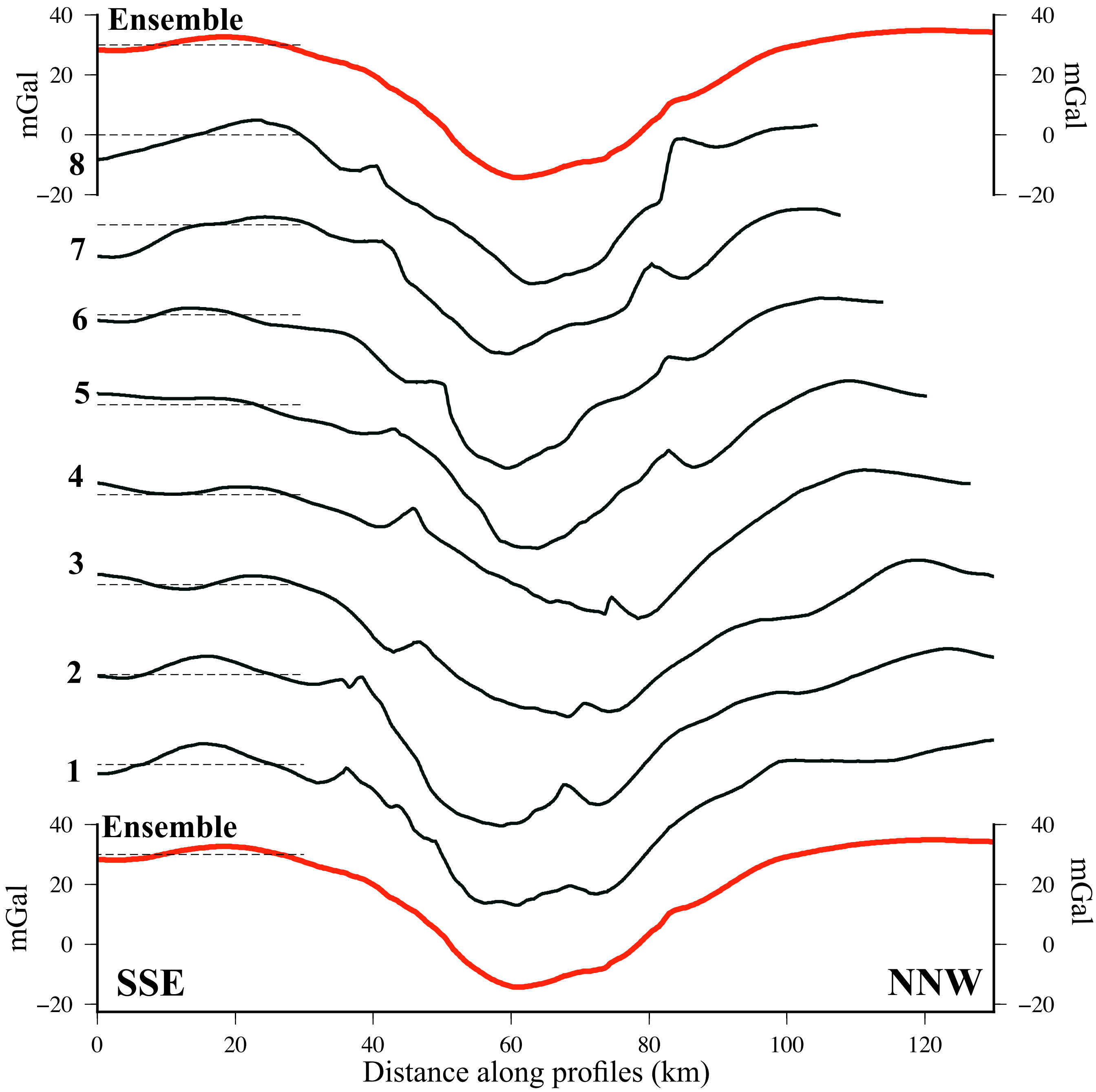

Ensemble
mGal
40
20
0
-20
8
7
6
5
4
3
2
1
SSE
NNW
0
20
40
60
80
100
120
Distance along profiles (km)

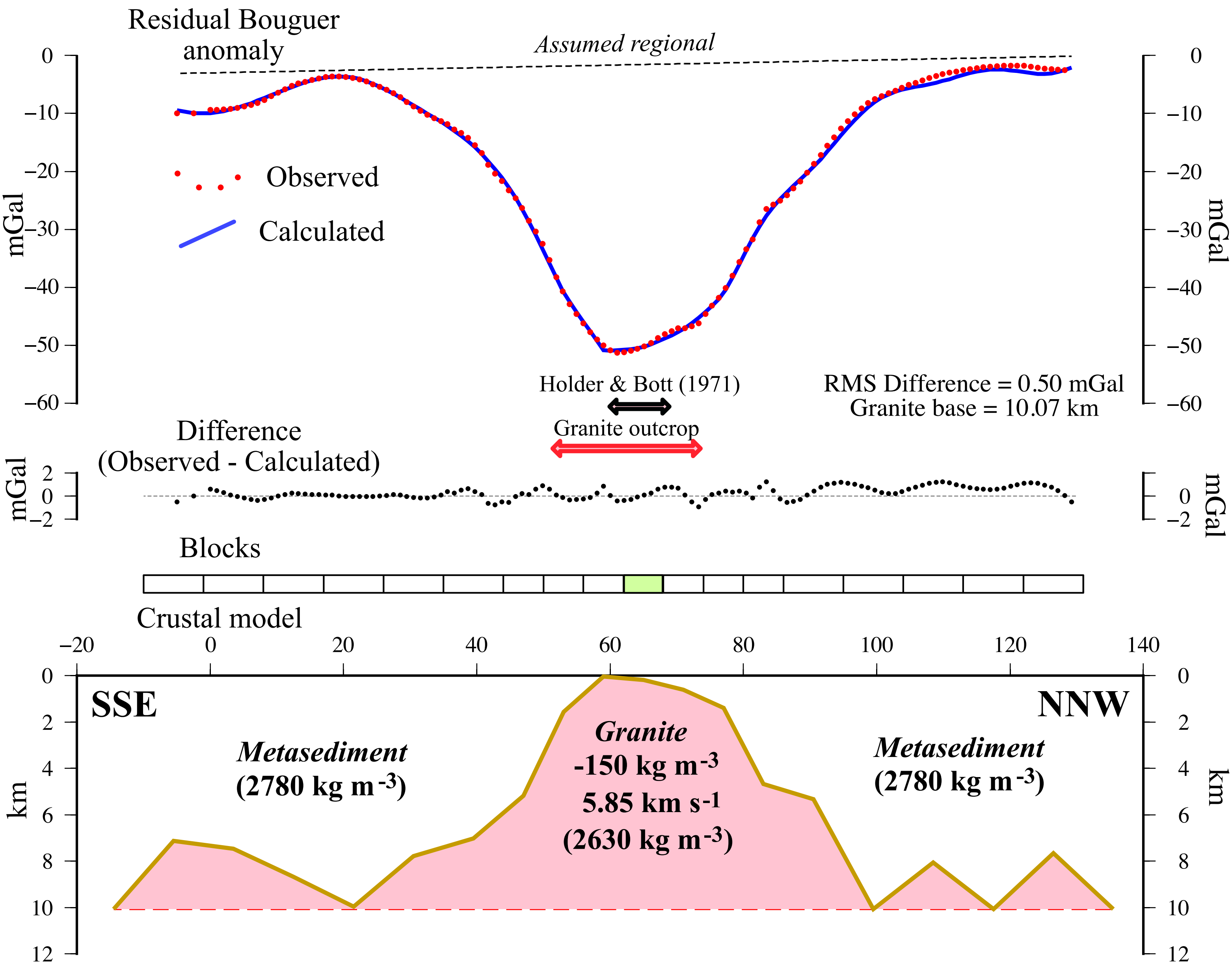
Residual Bouguer anomaly
Assumed regional
Observed
Calculated
mGal
0
−10
−20
−30
−40
−50
−60
Holder & Bott (1971)
Granite outcrop
RMS Difference = 0.50 mGal
Granite base = 10.07 km
Difference (Observed - Calculated)
2
0
−2
Blocks
Crustal model
−20
0
20
40
60
80
100
120
140
km
2
4
6
8
10
12
SSE
NNW
Metasediment (2780 kg m-3)
Granite -150 kg m-3 5.85 km s-1 (2630 kg m-3)
Metasediment (2780 kg m-3)

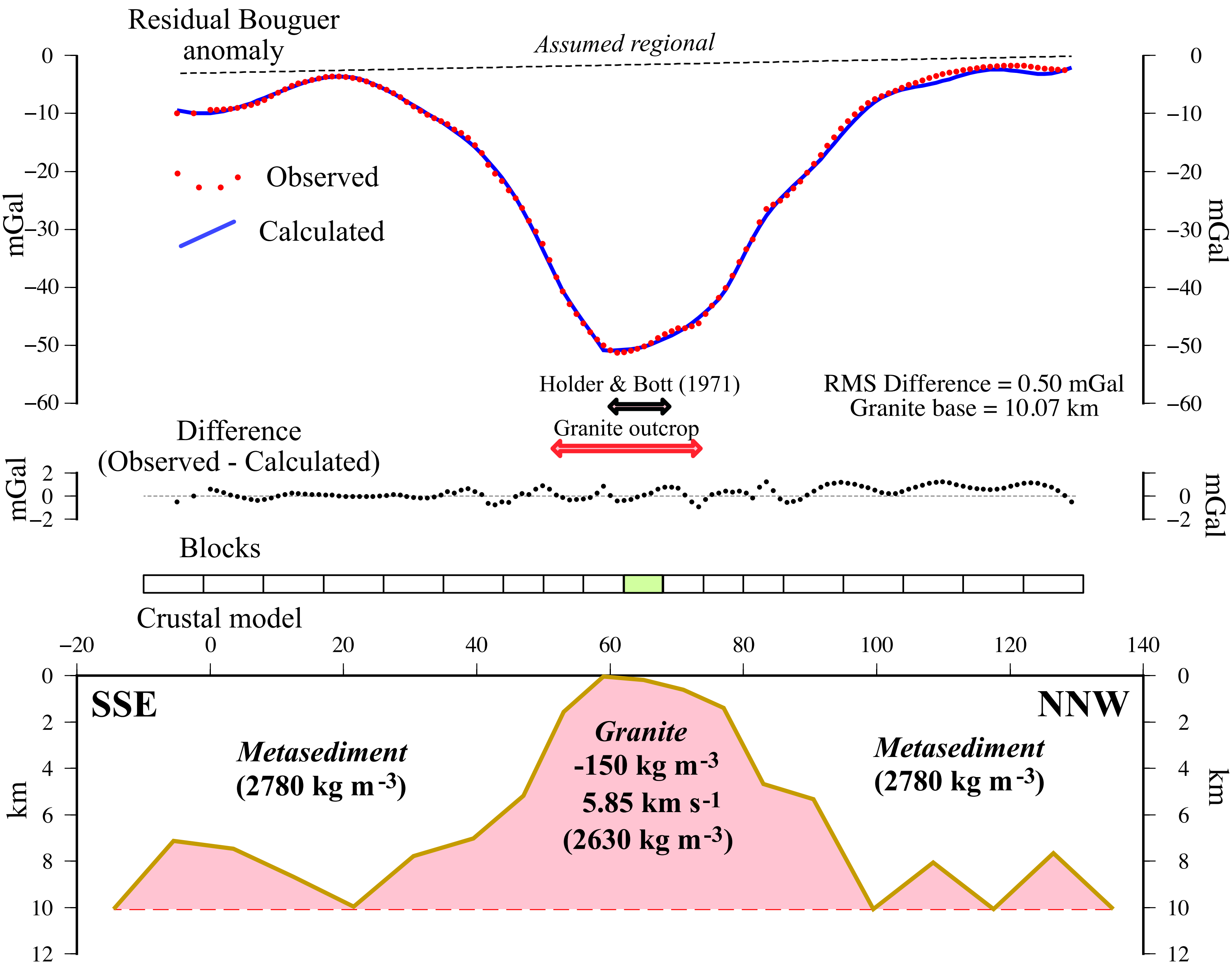

Residual Bouguer anomaly
Assumed regional
Observed
Calculated
mGal
Holder & Bott (1971)
Granite outcrop
RMS Difference = 0.50 mGal
Granite base = 10.07 km
Difference
(Observed - Calculated)
Blocks
Crustal model
SSE
NNW
Metasediment
(2780 kg m-3)
Granite
-150 kg m-3
5.85 km s-1
(2630 kg m-3)
Metasediment
(2780 kg m-3)
km

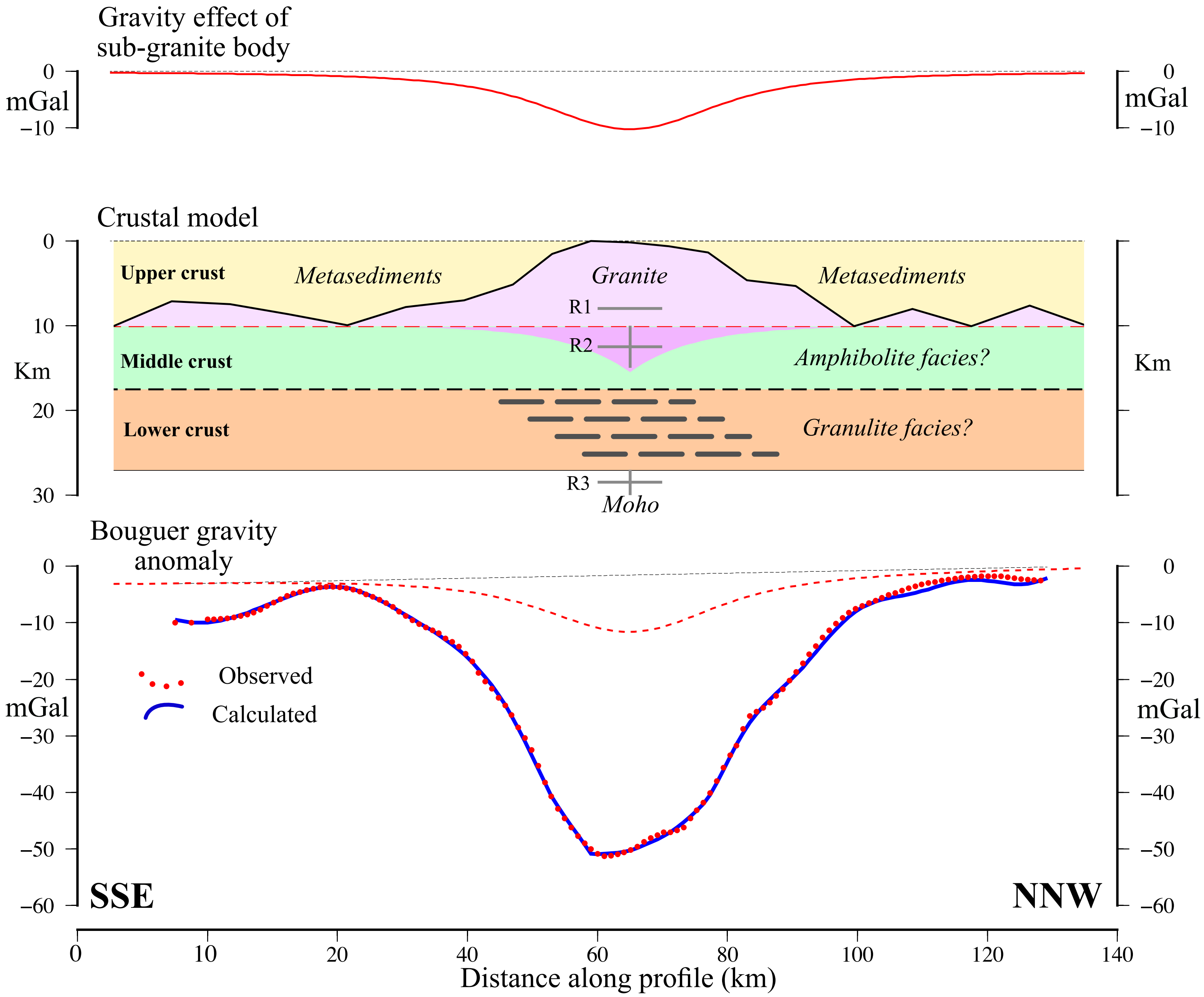

Gravity effect of sub-granite body
0
mGal
−10
Crustal model
Upper crust
Metasediments
Granite
Metasediments
R1
R2
Middle crust
Amphibolite facies?
Lower crust
Granulite facies?
R3
Moho
Km
0
10
20
30
Bouguer gravity anomaly
Observed
Calculated
mGal
0
−10
−20
−30
−40
−50
−60
SSE
NNW
0
10
20
40
60
80
100
120
140
Distance along profile (km)

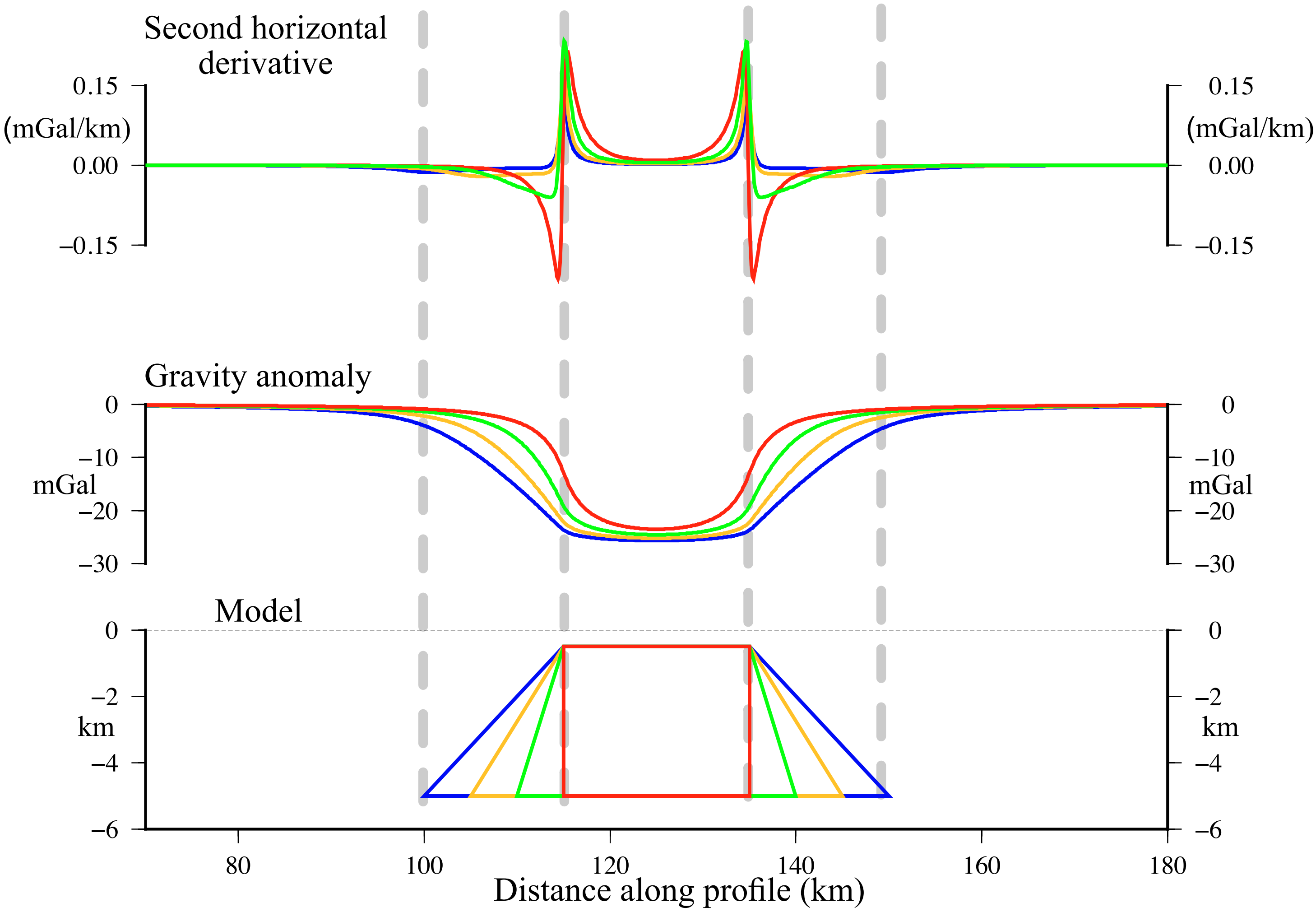

Second horizontal derivative
0.15
(mGal/km)
0.00
−0.15
0.15
(mGal/km)
0.00
−0.15
Gravity anomaly
0
−10
mGal
−20
−30
0
−10
mGal
−20
−30
Model
0
−2
km
−4
−6
0
−2
km
−4
−6
80
100
120
140
160
180
Distance along profile (km)

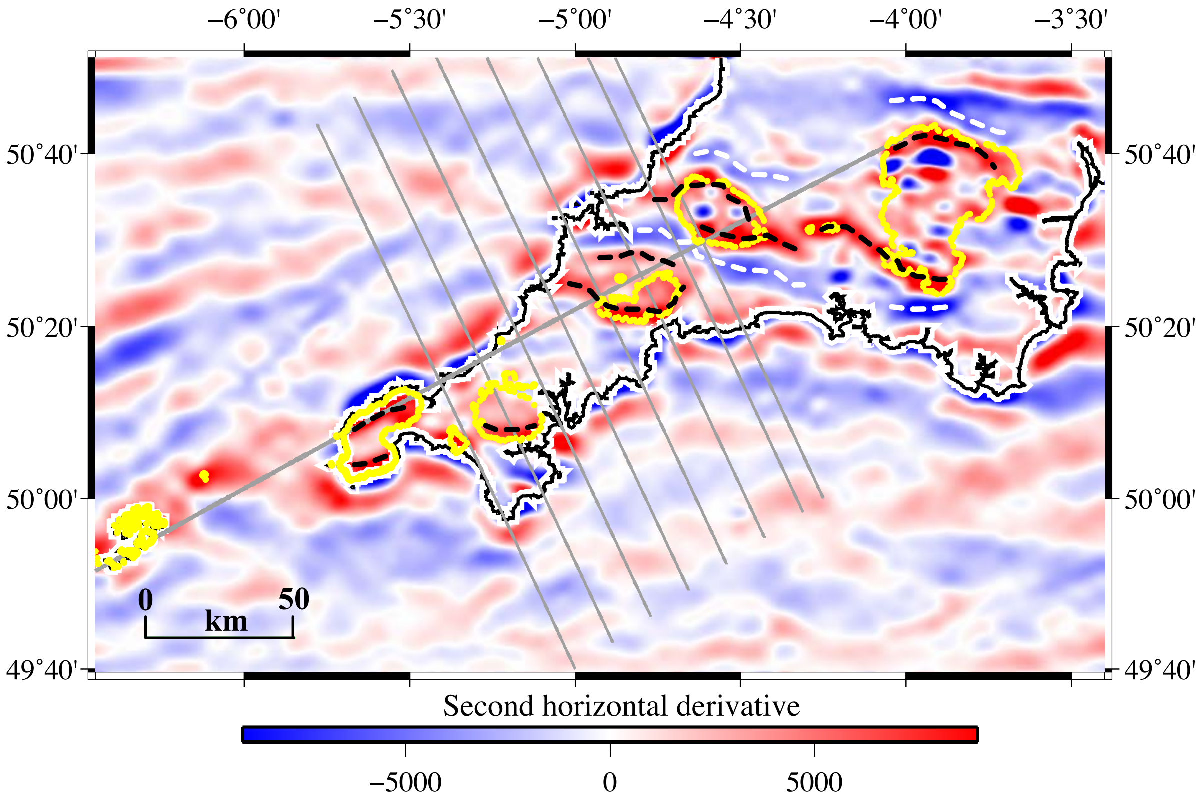

−6°00'
−5°30'
−5°00'
−4°30'
−4°00'
−3°30'
50°40'
50°20'
50°00'
49°40'
0
50
km
Second horizontal derivative
−5000
0
5000

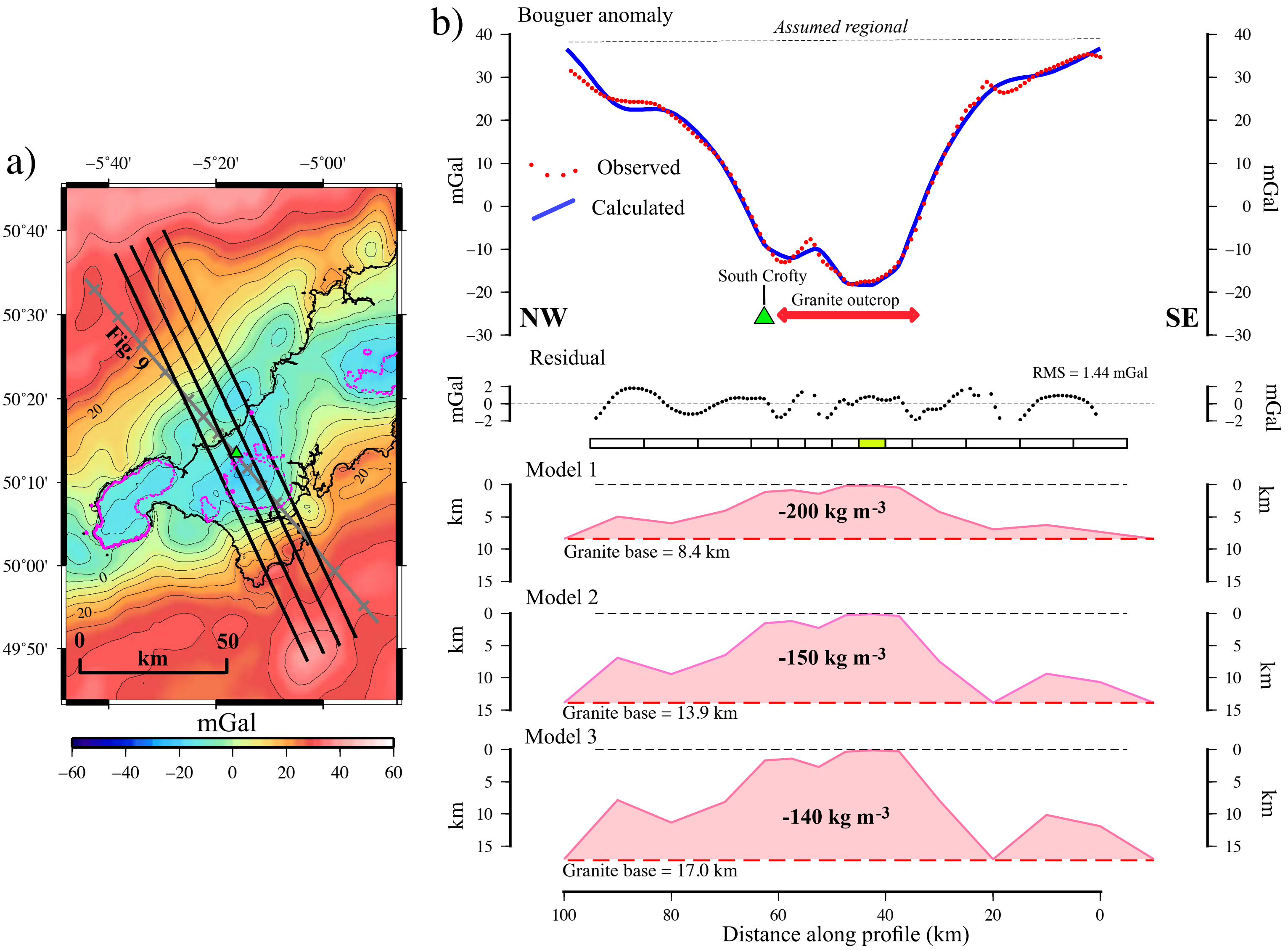
a)
–5°40'
–5°20'
–5°00'
50°40'
50°30'
50°20'
50°10'
50°00'
49°50'
Fig. 9
20
0
0
50
km
mGal
–60
–40
–20
0
20
40
60
b)
Bouguer anomaly
Assumed regional
mGal
Observed
Calculated
South Crofty
Granite outcrop
NW
SE
Residual
RMS = 1.44 mGal
Model 1
-200 kg m-3
Granite base = 8.4 km
Model 2
-150 kg m-3
Granite base = 13.9 km
Model 3
-140 kg m-3
Granite base = 17.0 km
km
Distance along profile (km)

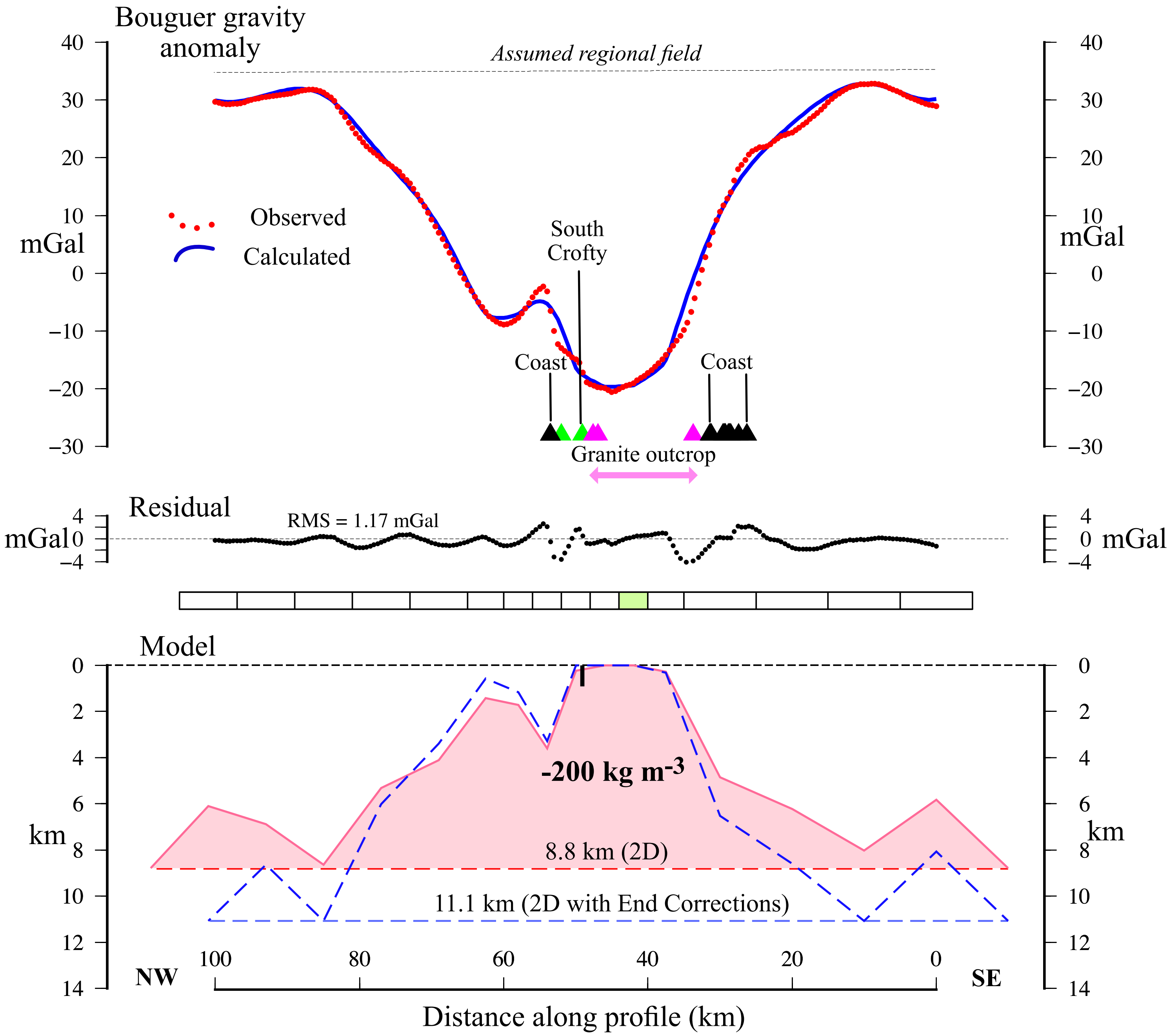

Bouguer gravity anomaly
Assumed regional field
Observed
Calculated
mGal
South Crofty
Coast
Coast
Granite outcrop
Residual
RMS = 1.17 mGal
mGal
Model
-200 kg m-3
8.8 km (2D)
11.1 km (2D with End Corrections)
km
NW
SE
Distance along profile (km)

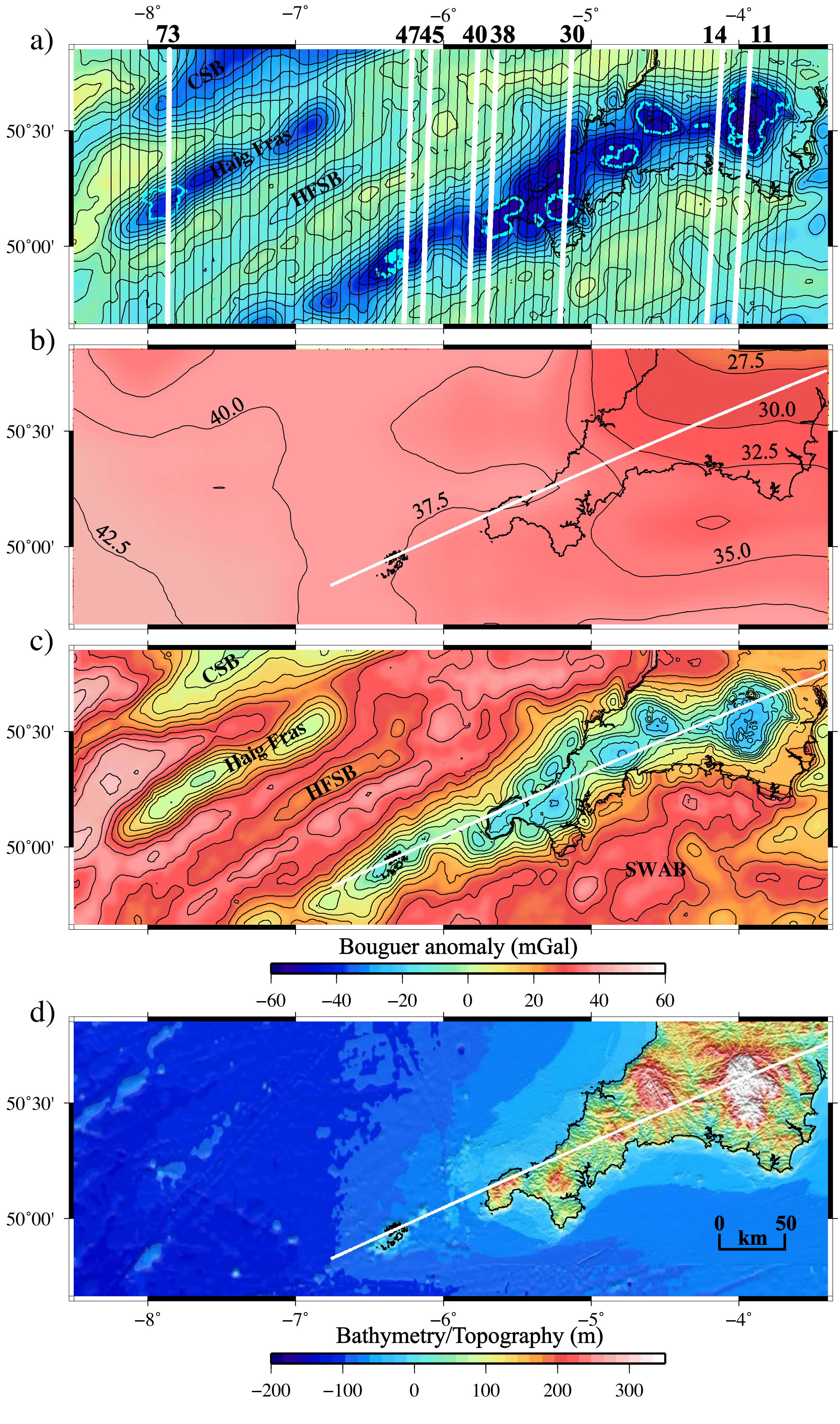

a)
73
47 45
40 38
30
14
11
CSB
Haig Fras
HFSB
b)
27.5
30.0
32.5
35.0
37.5
40.0
42.5
c)
CSB
Haig Fras
HFSB
SWAB
Bouguer anomaly (mGal)
−60 −40 −20 0 20 40 60
d)
0 50
km
−8° −7° −6° −5° −4°
50°30'
50°00'
Bathymetry/Topography (m)
−200 −100 0 100 200 300

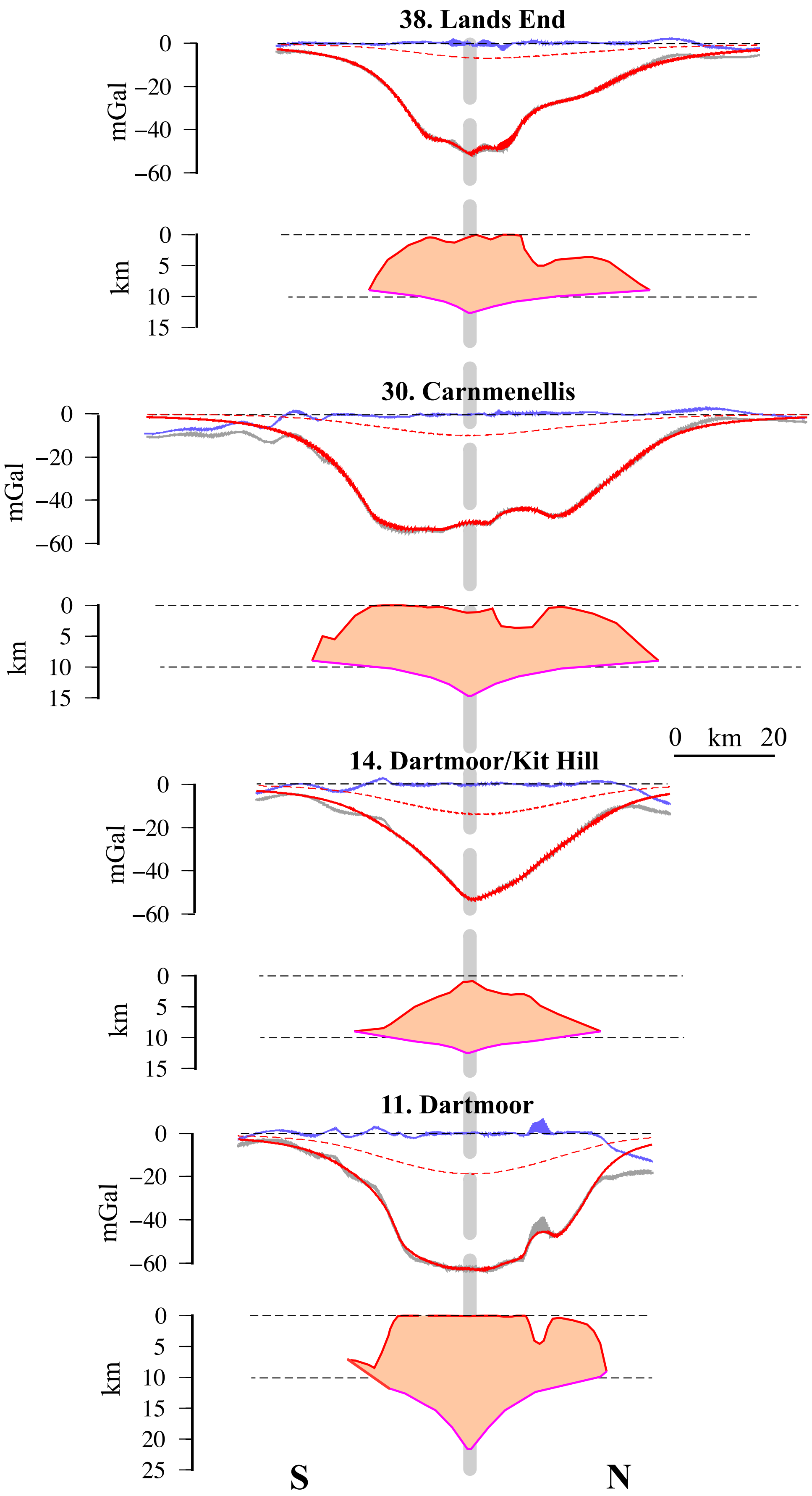

38. Lands End
mGal
km
30. Carnmenellis
0 km 20
14. Dartmoor/Kit Hill
11. Dartmoor
S
N

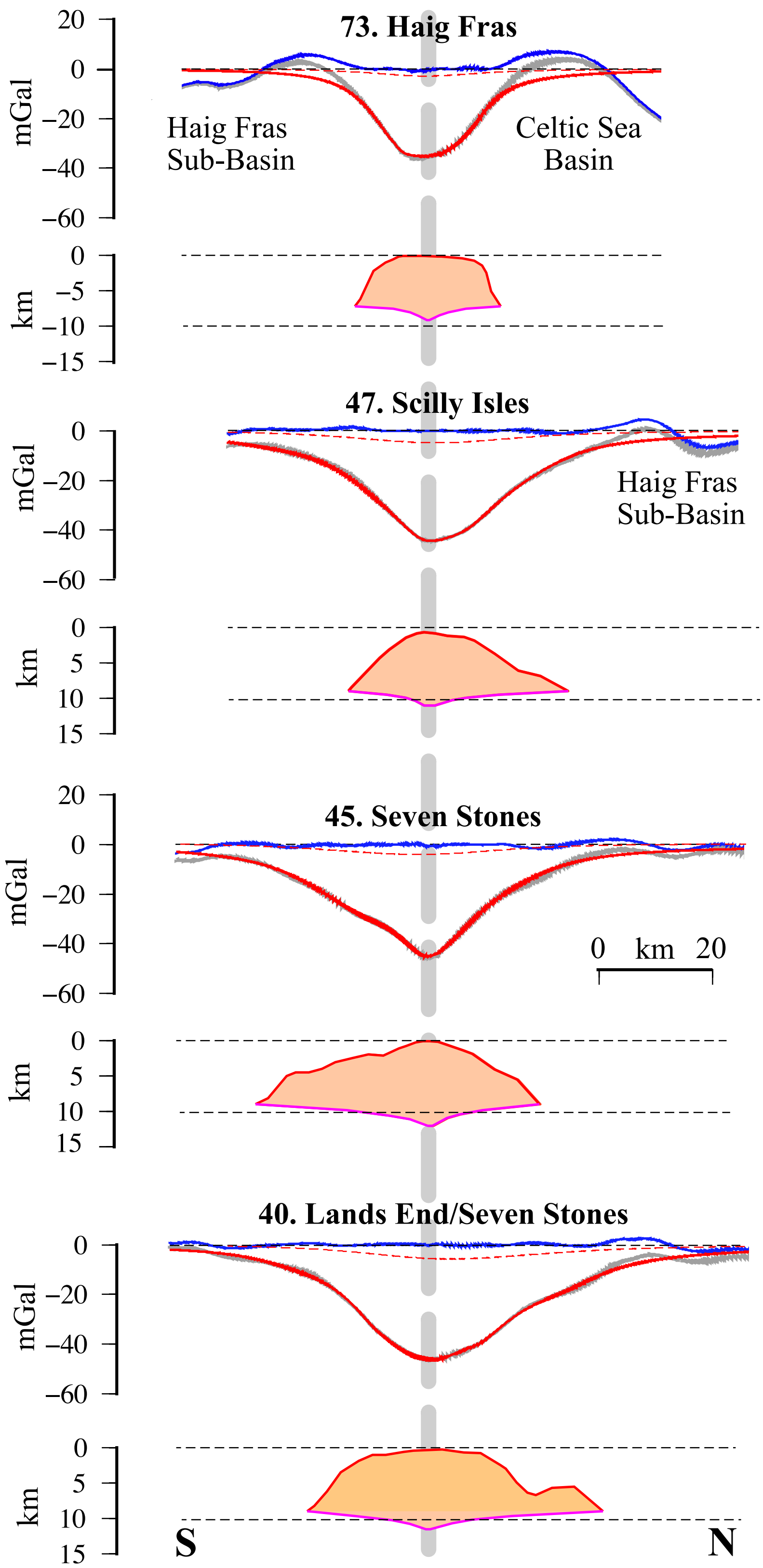

73. Haig Fras
mGal
km
Haig Fras
Sub-Basin
Celtic Sea
Basin
47. Scilly Isles
Haig Fras
Sub-Basin
45. Seven Stones
0 km 20
40. Lands End/Seven Stones
S
N

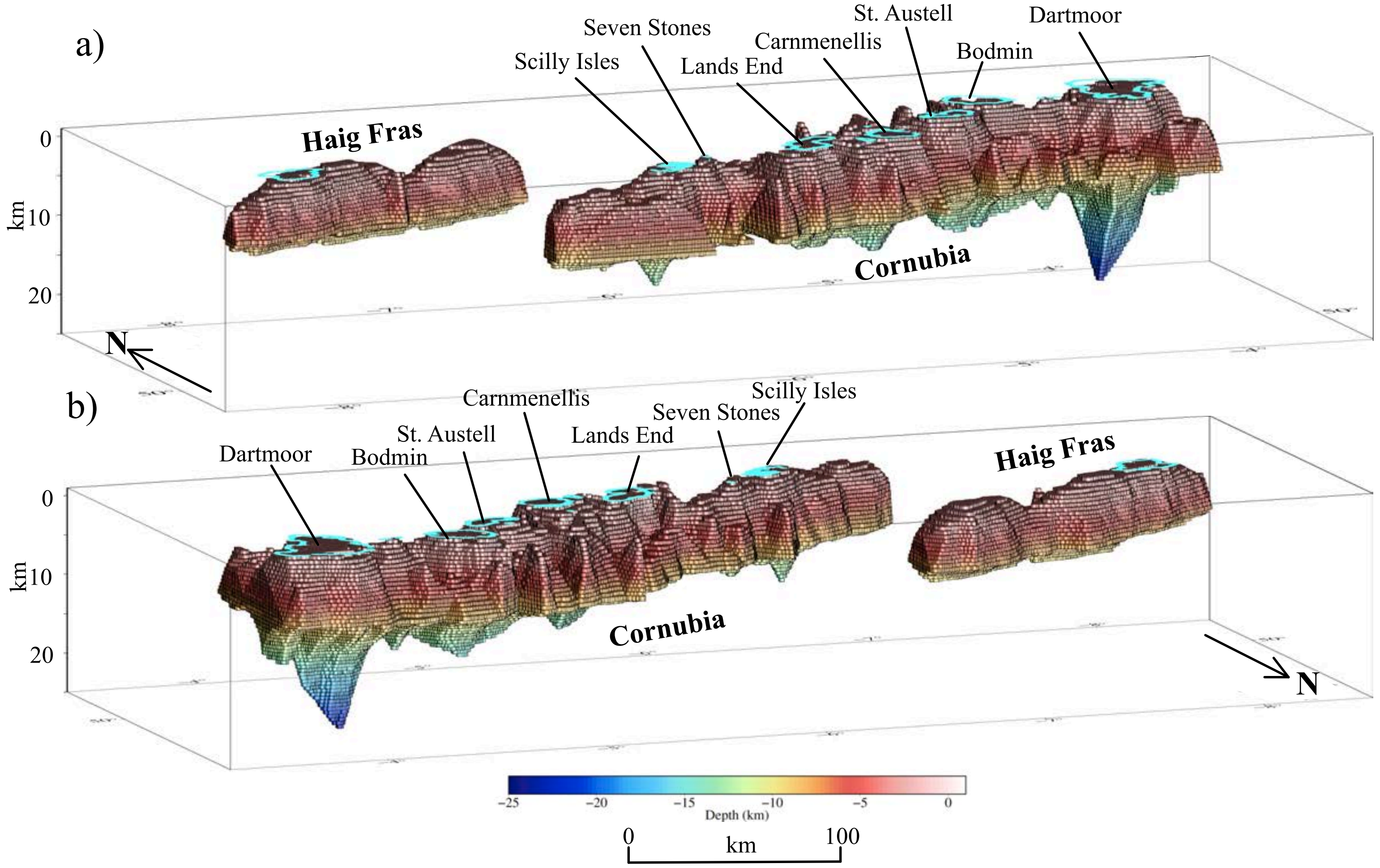

a)
Seven Stones
St. Austell
Dartmoor
Scilly Isles
Carnmenellis
Bodmin
Lands End
Haig Fras
0
km
10
20
Cornubia
N
b)
Carnmenellis
Scilly Isles
Seven Stones
St. Austell
Lands End
Dartmoor
Bodmin
Haig Fras
0
km
10
20
Cornubia
N
−25
−20
−15
−10
−5
0
Depth (km)
0
km
100

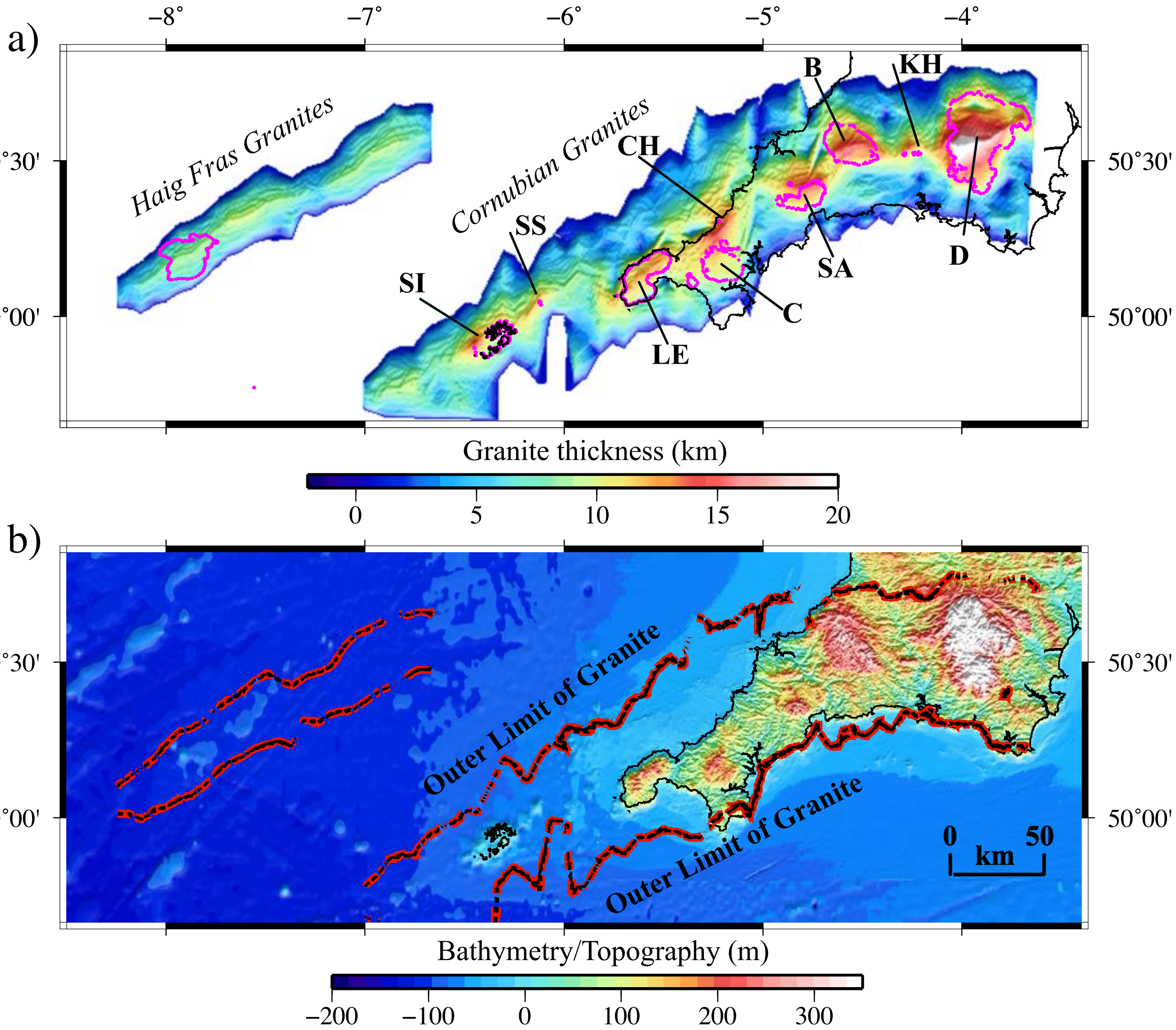
a)
–8°
–7°
–6°
–5°
–4°
50°30'
50°00'
Haig Fras Granites
Cornubian Granites
B
KH
CH
SS
SI
LE
C
SA
D
Granite thickness (km)
0
5
10
15
20
b)
Outer Limit of Granite
Outer Limit of Granite
0
50
km
Bathymetry/Topography (m)
–200
–100
0
100
200
300

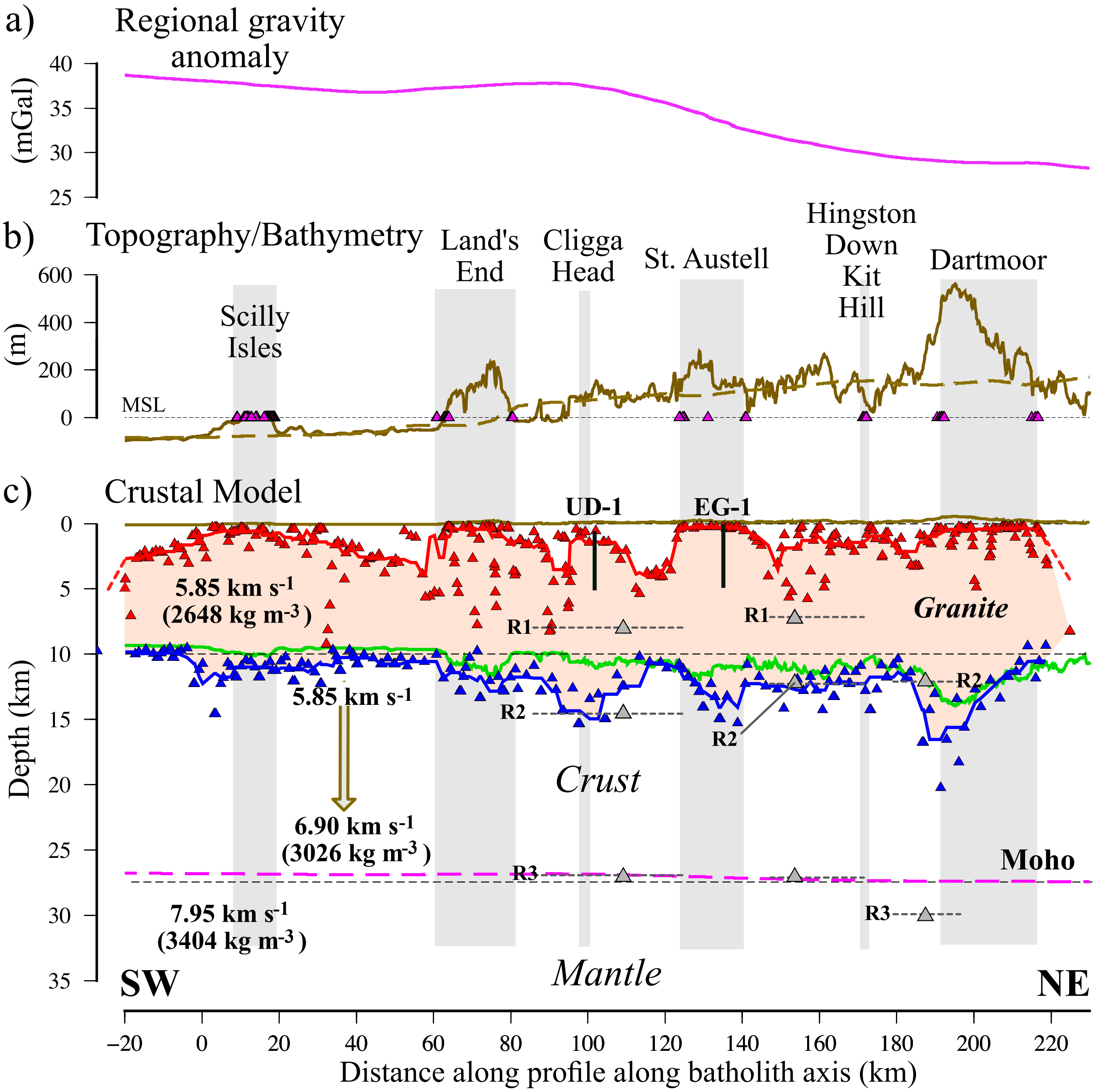

a) Regional gravity anomaly
(mGal)
40
35
30
25
b) Topography/Bathymetry
Scilly Isles
Land's End
Cligga Head
St. Austell
Hingston Down
Kit Hill
Dartmoor
(m)
600
400
200
0
MSL
c) Crustal Model
UD-1
EG-1
5.85 km s-1 (2648 kg m-3)
Granite
R1
R2
5.85 km s-1
Crust
6.90 km s-1 (3026 kg m-3)
Moho
R3
7.95 km s-1 (3404 kg m-3)
Mantle
SW
NE
Depth (km)
Distance along profile along batholith axis (km)

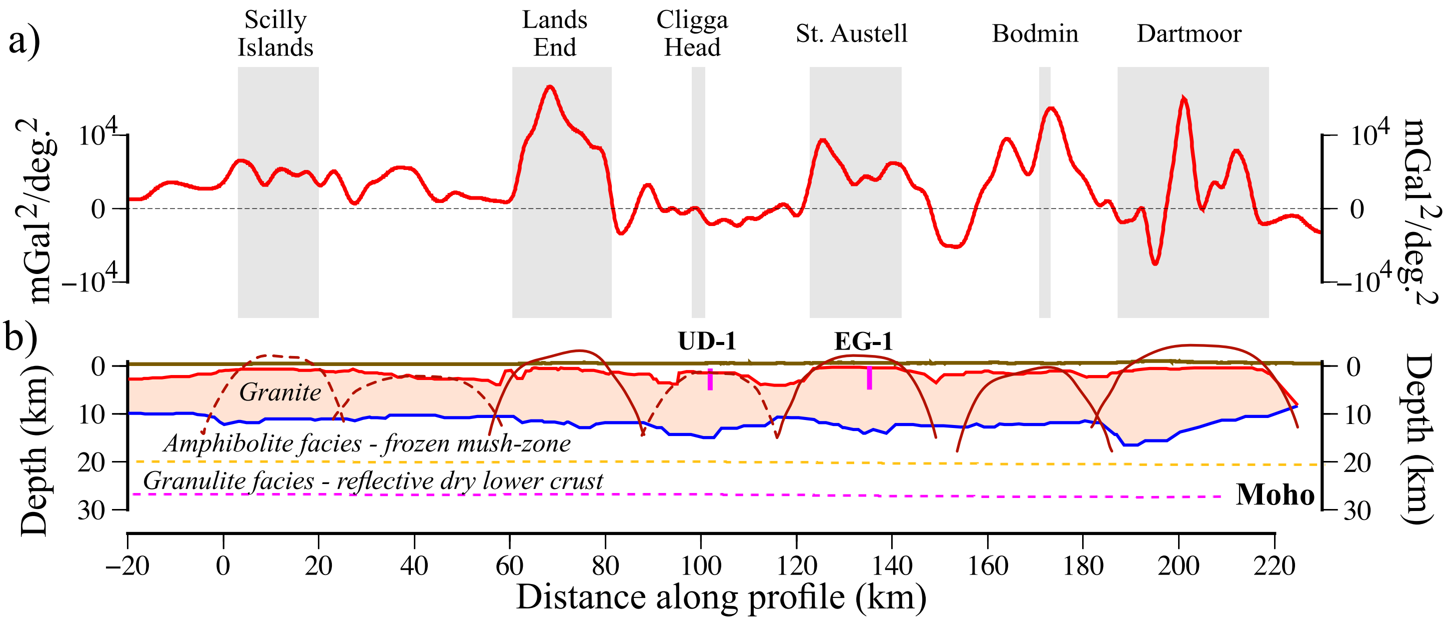

a)
Scilly Islands
Lands End
Cligga Head
St. Austell
Bodmin
Dartmoor
mGal²/deg.²
10⁴
0
−10⁴
b)
UD-1
EG-1
Depth (km)
0
10
20
30
Granite
Amphibolite facies - frozen mush-zone
Granulite facies - reflective dry lower crust
Moho
–20
0
20
40
60
80
100
120
140
160
180
200
220
Distance along profile (km)